CHANGE DETECTION AND DYNAMICS TOOLKIT (MONTH 18)

Deliverable D4.5.1

Circulation:	PU: Public
Lead partner:	UBO
Contributing partners:	UBO, IMATI, TU Delft
Authors:	André Stumpf, Romain Cancouët, Helen Piete, Christophe Delacourt (UBO) Michela Spagnuolo, Andrea Cerri (IMATI) Beril Sirmacek, Roderik Lindenbergh (TU Delft)
Quality Controllers:	Simon Julier (UCL)
Version:	1.0
Date:	30.04.2014

Consisting of

SINTEF	STIFTELSEN SINTEF, Department of Applied Mathematics, Oslo, Norway
Fraunhofer	Fraunhofer Institute for Computer Graphics Research, Darmstadt, Germany
CNR-IMATI-GE	Institute for Applied Mathematics and Information Technologies of the National Research Council (CNR-IMATI), Genova, Italy
MOSS	M.O.S.S. Computer Grafik Systeme GmbH (MOSS), Munich, Germany
HRW	HR Wallingford Ltd (HRW), Wallingford, UK
FOMI	Hungarian National Mapping and Cadastral Agency (FOMI), Institute of Geodesy, Cartography and Remote Sensing, Budapest, Hungary
UCL	University College London (UCL), Research centre for Photogrammetry, 3D Imaging and Metrology, London, UK
TUDelft	Delft University of Technology (TUDelft), Department of Geoscience & Remote Sensing & Man-Machine Interaction Group, Delft, The Netherlands
IGN	Institut National de l'Information Géographique et Forestière (IGN), Paris, France
UBO	Université de Bretagne Occidentale (UBO), European Institute for Marine Studies, Brest, France
Ifremer	L'Institut Francais de Recherche pour l´Exploitation de la Mer (Ifremer), Brest, France
Liguria	Regione Liguria, Genova, Italy

DOCUMENT HISTORY

Version[1]	Issue Date	Stage	Content and Changes
0.1	17/01/2014		Table of Contents – Draft 1
0.1.2	03/02/2014		Draft 1 – Added topological change detection
0.2	13/04/2014		Draft 2 – Added 2D displacement measurements
0.3	16/04/2014		Draft 3 – Incomplete draft, for checking by UCL
0.4	24/04/2014		Draft 4 –Material from IMATI, TU Delft integrated
0.5	25/04/2014		Draft 5 – Proof reading
0.6	27/04/2014		Quality Check
0.9	30/04/2014		Quality Check
1.0	30/04/2014		Final version submitted to Project Officer

[1] Integers correspond to submitted versions

EXECUTIVE SUMMARY

This document describes the development process, supporting libraries, and the first version of the IQmulus *Change Detection and Dynamics Toolkit* (D 4.5.1) as released in month 18 of the project (April 2014). It details three services for which prototypes have been implemented, documents the underlying algorithms and functionalities, and presents results of experimental tests on synthetic and real world datasets.

Considering the user requirements highlighted in D1.2.2 *Consolidated User Requirements* and the focus of the development within the IQmulus showcases in the domain of change detection, three services (Stochastic change detection, Topological change detection, and 2D displacement measurements) have been implemented. Besides the main analysis functionalities that are directly exposed to the user, the services comprise internal functions for data handling, resampling, and tiling. One of the three services can readily make use of multi-core parallelization and functionalities for visualization are available within the toolkit.

All services are furnished for the analysis of gridded data (typically GeoTIFF) and have been tested on relevant terrestrial and marine datasets. The characteristics of those test datasets are outlined briefly. Where relevant, state-of-the-art algorithms that are currently used for similar tasks have been evaluated and compared to the developed services.

Big data indicator	**Relevance**	**Explanation**
Volume	High	The scalability issue for the 3 services of the current toolkit is discussed in the sections 4.x.2. The outlook for future developments, especially for tackling very large data sets, is discussed in section 5.
Variation	High	The sample data sets used are described in section 3 and consist of VHR optical images and stereo point clouds, MBES digital terrain models, observed rainfall data and a low resolution digital terrain model, respectively.
Velocity	Medium	Computation times are addressed in the discussion of each service. While the toolbox comprises useful techniques for the analysis of bi-temporal datasets, the analysis of time series (in particular satellite images) has not been addressed yet but could be later in the project.
Analytics	High	All services in the toolkit extract valuable information about the dynamics of the given data sets: either by topological change detection, stochastic change detection or 2D displacement measurements using optical images.

TABLE: The relation between this report and the big data indicators

TABLE OF CONTENTS

1 INTRODUCTION

This document presents the progress of Task 4.5 on change detection and dynamics during the first 18 months of the IQmulus project. It describes the development process, underlying libraries, the functionalities and parameters of developed service prototypes, and the results of a series of tests that were performed on several real-world datasets. The services being developed under Task 4.5 are currently:

- Service 45: Topological Change Detection
- Service 53: Stochastic Change Detection
- Service 60: 2D displacement measurement using DSM/DTM/DEM and optical images

Those services are complex services building on gridded date representations (e.g. output of other algorithms such as surface interpolation and outlier detection) and comprise several internal processing steps such as grid resampling and masking.

Service 45 targets a topological analysis (*0th persistence*) of a distance map obtained from two co-registered gridded point clouds (GeoTIFF). Maxima, minima and saddles of such maps are used to detect and encode its topological changes, and rank them by importance. Furthermore, points at which topological changes occur can be detected. A future service release will be able to deal with triangulations (.ply).

Service 53 targets the statistical detection of significant changes between two surfaces taking into account the uncertainty of the input dataset and a normal distribution of the inherent errors. The detection results are provided as a binary image indicating stability vs. change and additionally as a grayscale GeoTIFF representing stability of the change metric as the distance to the error model.

Service 60 is the first release of an image correlation algorithm to quantify displacement among two optical images or numerical surface models with sub-pixel accuracy. The service builds upon an existing open-source library and implements a hierarchical window-based approach for image matching based on normalized cross-correlation and spatial regularization. The service is parallelized and includes basic tools for visualization. Further work is required to transfer the parallelization into the IQmulus cloud environment.

The three services are complementary since they target different types of changes (topological changes, vertical changes, horizontal changes).

All three services were evaluated processing IQmulus datasets and additional datasets available to the mainly involved institutional partners (UBO, IMATI, TUDelft). The evaluation was carried out with respect to the performance indicators defined for the toolkit in D4.1.2. :

- Quality (precision, robustness, etc.)
- Scalability (Computational runtime, memory consumption, etc.)
- Degree of human intervention (Number and sensitivity of free algorithm parameters)

1.1 RELATED SHOWCASES AND USER STORIES

The detection and quantification of changes from heterogeneous multi-temporal geospatial data is crucial to understand and monitor environmental changes. The current development in Task 4.5 targets the detection of surface changes in marine and terrestrial environments and is therefore directly related to both the land and the marine show case.

Land showcase:

"As hydrologist/ geomorphologist supporting decision makers in civil protection, I want to analyse data measured during critical events to prepare better prediction and monitoring of floods and landslides. To this end, ***I want to study the evolution of measured precipitation data as well as slope deformation from optical images****, compute parameters to produce high-quality input for hydrological and mechanical modelling and simulation, and compare the results to reference measurements obtained for flooding events and landslides."*

Marine showcase:

"As an engineer/scientist I want to create a seamless land/underwater elevation model by the integration of any data sources for elevation. I want to create the model 'on demand' and bespoke to my requirements, in particular which datasets to use as input. ***In addition I would like to identify bathymetric features in the data, including their associated dynamics (e.g. movement of sand waves).*** *The data sources available will include topographic and bathymetric LIDAR and SONAR point clouds and existing digital elevation models and surface models. They will be in different data formats, data models, and have different spatial and temporal representations of elevation."*

User stories currently addressed within Task 4.5:

- 1.2.1_50: I want to be able to derive landslide parameters (geometry / speed / volume / depth / type etc.) from multi-temporal aerial photography and DTM data
- 1.2.1_51: I want to monitor the shoreline regarding: erosion rate, mass budget, etc.
- 1.1_52: As a hydrologist, I want to extract significant break lines from high resolution DTMs or point clouds, such as dikes, dams, banks, ditches so that I can improve my hydraulic model and make more accurate simulations.
- 1.2.1_75: I would like to have tools to study the dynamics of sediments in the seafloor (volumes of sediments moved in temporal series).
- 1.2.1_73: As a GIS expert for coastal monitoring, I would like to have tools for the analysis of the geomorphology of the seafloor.

2 LIBRARIES, PROGRAMMING LANGUAGES AND METHODS

This section provides an overview of generic libraries, software tools and programing languages that currently support the development of services within the change detection and dynamics toolkit. The supporting development tools have been selected after an extensive review of available tools carried out by all WP4 partners involved. The set of tools will be extended further according to the needs of future implementations.
Where applicable we also provide an overview of already available methods and implementations that address surface change detection with similar objectives and compare their performance briefly with the services furnished under Task 4.5.

2.1 STOCHASTIC CHANGE DETECTION

This section provides an overview of the libraries that were used for the development of Service 53 comprising Eigen, Boost, VTK, and OpenCV. In addition, LibGeoTIFF and LibTIFF, which are described in section 2.2.1 and 2.2.2, respectively, were also used for the development. The numbers of the currently used versions are given in parentheses.

2.1.1 Eigen C++ Library (3.2.1)

Eigen is a C++ library of template headers that implements linear algebra and related matrix operations.

2.1.2 Boost C++ Library (1.55.0)

Boost is a set of libraries for the C++ programming language that provide support for tasks and structures such as linear algebra, pseudorandom number generation, multithreading, image processing, regular expressions and unit testing. Boost is required by libLAS and PCL, and it is also used by commercial packages including Matlab and Adobe Acrobat. The libraries are mostly released under the Boost Software License, which allows for the use of the libraries in commercial products. Given its widespread use by multiple IQmulus partners this library will be used throughout the duration of the project.

2.1.3 VTK C++ Library (6.1)

VTK is an open source framework for 3D computer graphics, image processing and visualization. VTK supports a wide variety of visualization algorithms including scalar, vector, tensor, texture and volumetric methods and advanced modelling techniques such as implicit modelling, polygon reduction, mesh smoothing, cutting, contouring, and Delaunay triangulation.

2.1.4 OpenCV C/C++ Library (2.4)

OpenCV is a library of programming functions mainly aimed at real-time computer vision. The OpenCV library's wide solution spectrum includes functions for 2D and 3D feature extraction, segmentation, stereo vision, classification and learning methods.

2.2 TOPOLOGICAL CHANGE DETECTION

In what follows we provide a brief description of the libraries which have been adopted to develop Service 45: Topological Change Detection. For the first release, the service targets the

analysis of gridded point clouds in the form of GeoTIFF files, thus building on the LibTIFF and the LibGeoTIFF libraries. Furthermore, the ShapeLib Library has been used to enable the storage of additional information as ESRI Shapefiles.

2.2.1 LibTIFF C/C++ Library (4.0.3)

LibTIFF is a set of C functions supporting the manipulation of TIFF image files. The library requires an ANSI C compilation environment for building and presumes an ANSI C environment for use.

LibTIFF provides interfaces to image data at several layers of abstraction. At the highest level image data can be read into an 8-bit/sample, ABGR pixel raster format without regard for the underlying data organization, color space, or compression scheme. Below this high-level interface the library provides scanline-, strip-, and tile-oriented interfaces that return data decompressed but otherwise untransformed. These interfaces require that the applications first identify the organization of stored data and select either a strip-based or tile-based API for manipulating data. At the lowest level the library provides access to the raw uncompressed strips or tiles returning the data exactly as it appears in the file.

2.2.2 LibGeoTIFF C/C++ Library (1.4.0)

LibGeoTIFF is a library built on top of LibTIFF for reading and writing coordinate system information from/to GeoTIFF files. It includes CSV files for expanding projected coordinate system codes into full projections, and definitions and examples of transforming the definitions into a form that can be used with the PROJ.4 projections library. It also includes the sample applications listgeo (for dumping GeoTIFF information in readable form) and geotifcp (for applying GeoTIFF tags to an existing TIFF or GeoTIFF file).

2.2.3 ShapeLib C/C++ Library (1.3.0)

The ShapeLib Library provides the ability to write simple C programs for reading, writing and updating (to a limited extent) ESRI Shapefiles, and the associated attribute file (.dbf).

2.3 2D DISPLACEMENT MEASUREMENT

This section provides an overview of selected image correlation algorithms that are currently most commonly used for geoscientific applications and operational monitoring as well as libraries that were used for the elaboration of a processing service adapted mainly for land and marine applications.

2.3.1 CIAS – Correlation image analysis (version 23 May 2013)

CIAS has been initially developed by (Kääb and Vollmer 2000) for measurements of glacier flow from multitemporal aerial photographs in alpine environments and has since been modified and applied in many glaciological studies using aerial and satellite images (Heid and Kääb 2012; Kääb 2004). The corresponding algorithms are implemented in IDL (Exelis) and available as compiled libraries that require IDL which is proprietary but freely available. The main algorithm performs a window-based search to determine the match between a reference image and a test image using normalized cross-correlation as a matching criterion. The position of the matching peak is refined to sub-pixel accuracy matching the correlation peak by fitting a parabolic function to the correlation surface. The library further implements orientation-correlation (Fitch

et al. 2002), which computes x and y components of the orientation of the image gradient at each pixel location that are subsequently used as an input for the described correlation algorithm.

2.3.2 CNES correlator (no version information available)

This matching algorithm has been developed at Centre National des Etudes Spatial using IDL (Vadon and Massonnet 2000) and has been used in a number of studies to measure for example glacier displacement (Berthier et al. 2005), coseismic slip (Feigl et al. 2002) and landslide deformation (Delacourt et al. 2004). The algorithm performs window-based matching directly on the intensity values of the input images and uses a least squares approach to maximize the correlation function. Sub-pixel precision is reached through an iterative resampling of one of the two images with a sinc interpolation. The code was made available to us for a limited time and is not intended for public use.

2.3.3 CosiCorr (release 2010-01-08)

CosiCorr is an IDL library implementing among other tools a sub-pixel image matching technique that operates in the frequency domain. The technique was developed at the California Institute of Technology (Leprince et al. 2007) and the compiled library is available freely for download. The execution of the library requires ENVI (Exelis) which is proprietary software for image processing. The method also follows a window-based approach but matching is performed through phase correlation after a Fourier transform with sub-pixel precision. A scheme for masking high frequencies from the normalized cross-spectrum additionally provides better robustness to noise and a hierarchical sequence with iteratively decreasing window size can be used to measure large displacement. The implemented algorithm can be considered as the current state of the art and is widely used in studies of coseismic slip, glacier monitoring or the investigation of sand dunes (e.g., Barisin et al. 2009; Necsoiu et al. 2009; Scherler et al. 2008).

2.3.4 C++ correlator (MICMAC, revision 333307)

MICMAC is an open source project hosted at IGN-France (Deseilligny et al. 2013) and dedicated to surface reconstruction from stereo- and multi-view terrestrial, aerial and satellite images. Among several tools for tie point detection, image orientation and dense reconstruction the library comprises an hierarchical image correlation algorithm which was originally designed for surface reconstructions from aerial photographs (Pierrot-Deseilligny and Paparoditis 2006) and only recently has been adapted to derive coseismic displacement (Rosu et al. 2014). Yet it has not been tested for cloud-based processing of large volume image datasets. The algorithm performs a window-based search using normalized cross-correlation as matching criterion and allows imposing a spatial regularization to control the smoothness of the displacement field. The algorithm follows a hierarchical scheme and allows for sub-pixel precision by interpolation of the input images using a windowed sinc function.

2.3.5 R (3.1)

R is an open-source software environment for statistical computing and graphics. It comprises core functionalities for statistical analysis and modelling as well as several hundred contributing packages including libraries for parallel processing as well as handling, analysis and visualization of spatial data. In the context of Task 4.5 R is currently used to implement routines for the filtering of the derived displacement fields and the visualization of the resulting vector fields. The developed functions depend on the following contributing packages:

- rgdal (0.8-16) – Bindings to the geospatial data abstraction library
- raster (2.2-31) – Geographic raster analysis and modelling
- rasterVis (0.27) – Visualization methods for raster data
- XML, r-cran-xml (3.98 – 1.1) – Tools for parsing and generating XML
- CircStats (0.2 -4) – Tools for circular statistics
- Mixtools (1.0.1) – Tools for analysing finite mixture models
- SDMTools (1.1-20) – Includes tools for converting raster format data
- Adehabitat (1.8.12) – Includes tools for mathematical morphology

2.4 GENERAL PURPOSE LIBRARIES

GDAL (1.10.0-1): The geospatial data abstraction library for reading, resampling and writing raster data

Tcl-tk/ tk-dev (8.5): Tool command language for the development of graphical user interfaces

GNU make (3.81- 8.10): Tool for compilation and parallelization at runtime

GCC (4.6.3-1 or higher): GNU compiler for C/C++

Imagemagick (6.6.9.7): Image manipulation tools

libimage-exiftool-perl: Library and program to read and write meta information in multimedia files

exiv2 (0.22-2): Tool for the manipulation of image metadata

libgeo-proj4-perl (1.05-1): Proj4 libraries for geographic projections

3 DATA SETS

The subsequent sections describe the main data sets that were used during the development for functional testing and evaluation. Details regarding the source, extent, size and potential use of the datasets are provided.

3.1 VHR OPTICAL IMAGES AND STEREO POINT CLOUDS (LANDSLIDES, FRENCH ALPS), ID 38-39

The Pléiades satellites constellation comprises two sun-synchronous polar-orbiting satellites with a phase shift of 180°. The satellites capture optical images in 4 multi-spectral (blue, red, green, near-infrared) and one panchromatic band (Figure 2) at a nominal resolution of 2 m and 0.5 m. The high agility of the system enables to capture images with short repeat pass cycles (<5) and with monoscopic, stereoscopic, and multi-view geometries.

The dataset comprises a series of panchromatic and multispectral images that were captured over the Barcelonnette area (Southern French Alps) between spring 2012 and autumn 2013 and cover an area of 160 km^2. Several active landslides exist in the area and require continuous monitoring with ground-based and remote sensing techniques. Commercial software (Erdas LPS 2013) was used to generate 3D point clouds from multiple stereo-pairs and corresponding orthoimages which can serve as input for the services in the toolkit. The services are aimed to detect and to quantify different components (e.g. horizontal, vertical) of the surface deformation.

A preliminary accuracy assessment of the 3D point clouds (Table 1) was carried out on subsets of the data where airborne LiDAR scans were available and allowed to gain insights into the uncertainties of this dataset. For this purpose the point clouds where interpolated into a gridded raster. The analysis revealed that the spatial distribution of errors is closely linked to the surface characteristics. The mean absolute error (MAE) amounts up to 3m (mainly related to shaded areas, vegetated and steep slopes, Figure 1a) but is significantly lower (MAE = 0.74 m) at locations with gentle slopes and sparse vegetation (Figure 1b).

TABLE 1: DETAILS ON THE FRENCH ALPS 3D POINT CLOUD DATA SET

Type	Date	pts.m^{-2}	Total area	Size	IQmulus Metadata ID
3D points	05 Oct 2012	1 – 4	~ 100 km^2	2.6 GB	38
3D points	31 Jul 2013	1 – 4	~ 100 km^2	2.7 GB	38
3D points	21 Sept 2013	1 – 4	~ 100 km^2	3.9 GB	38

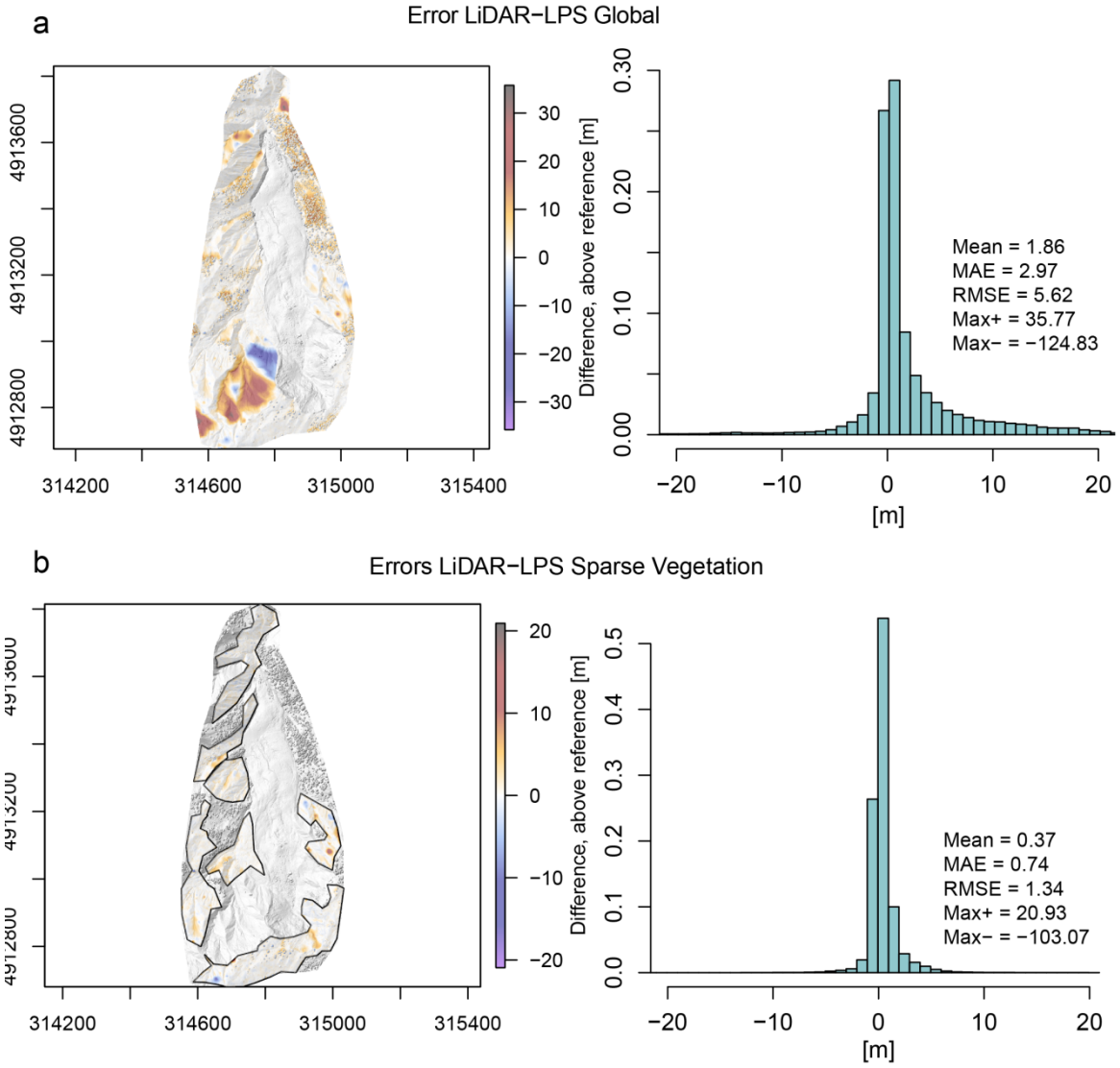

FIGURE 1: ACCURACY ASESSMENT OF THE SURFACE MODELS GENERATED FROM PLÉIADES STEREO-PAIRS AGAINST AIBORNE LIDAR SCANS. (A) GLOBAL ERROR AT THE SUPER SAUZE LANDSLIDE AND (B) ERRORS OVER SPARSELY VEGETATED AREAS (MARKED WITH BLACK OUTLINES).

The extracted surface models were used to orthorectify the panchromatic images at a resolution of 0.5 m. Details on the orthorectified images are provided in Table 2. As illustrated in Figure 2 the co-registration of the orthoimages provides sub-pixel accuracy (RMSE < 0.16 cm).

TABLE 2: DETAILS ON THE FRENCH ALPS ORTHOIMAGE DATA SET

Type	Date	Resolution	Total area	Size	IQmulus Metadata ID
Orthoimage	07 Aug 2012	0.5 m	~ 100 km²	0.9 GB	39
Orthoimage	05 Oct 2012	0.5 m	~ 100 km²	0.9 GB	39
Orthoimage	31 Jul 2013	0.5 m	~ 100 km²	1.8 GB	39
Orthoimage	21 Sept 2013	0.5 m	~ 100 km²	1.8 GB	39

FIGURE 2: SIDE-BY-SIDE VIEW OF TWO ORTHOIMAGES ILLUSTRATING THE HIGH QUALITY OF THE CO-REGISTRATION. THE IMAGE DEPICTS PARTS OF A SUBURBAN NEIGHBORHOOD AT BARCELONETTE (SOUTH FRENCH ALPS) ON OCT 2012 (LEFT) AND AUG 2012 (RIGHT).

3.2 MBES DTMS (SUBMARINE DUNES, BRITANNY), ID 12-13

This dataset was derived from three bathymetric surveys (Table 3) of the Banc de Four (offshore Western Britanny) using multi-beam echo soundings (MBES). The dune field at Banc de Four is highly dynamic and precise measurements of the dune migration are required to better quantify and understand the sediment transfer in the system and its relations with tidal currents.

TABLE 3: DETAILS ON THE BANC DE FOUR BATHYMETRY DATASETS

Type	Date	Resolution	Total area	Size	ID
DTM	Feb 2009	4 m (xy) and 0.01 m (z)	~ 140 km²	50 MB	12-13
DTM	Aug–Sept 2010	2 m (xy) and 0.02 m (z)	~ 10 km²	40 MB	12-13
DTM	Jul 2011	2 m (xy) and 0.02 m (z)	~20 km²	80 MB	12-13

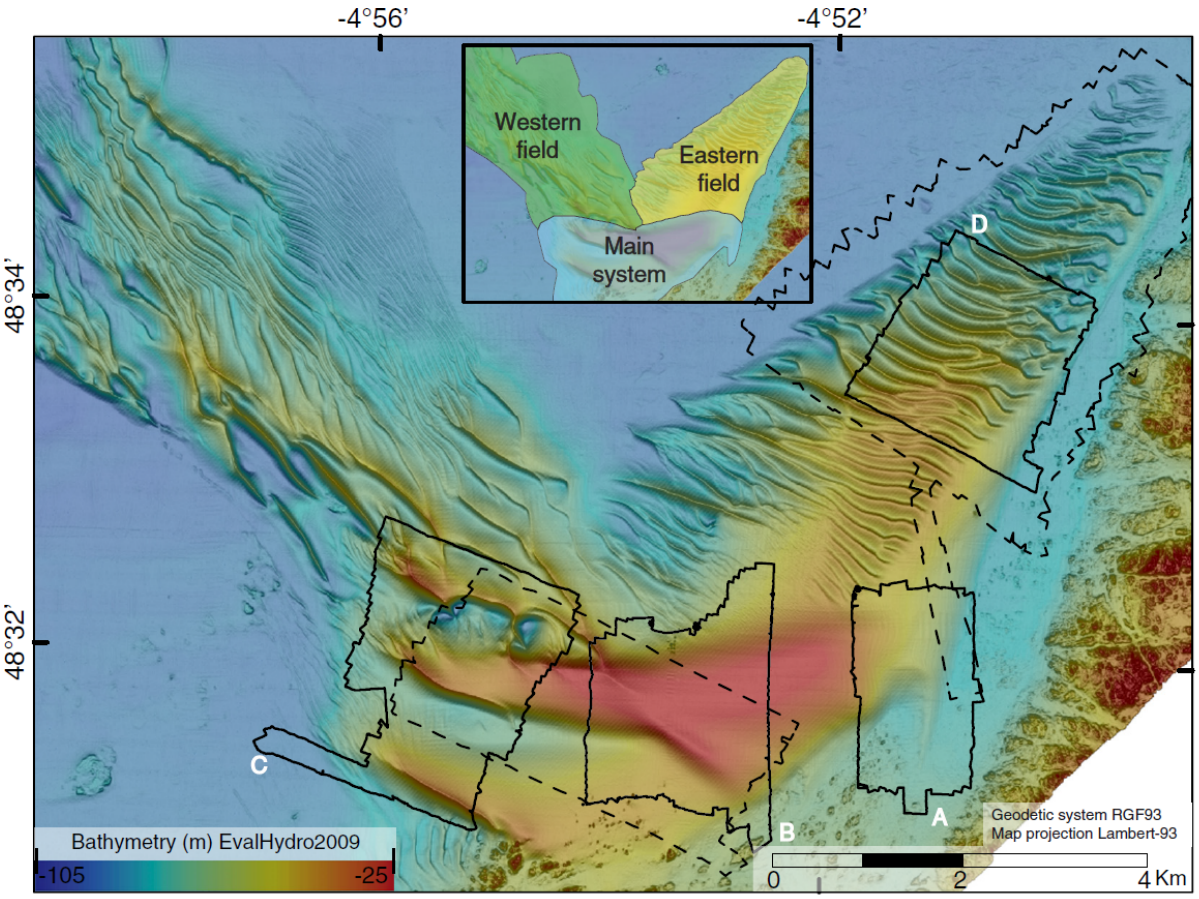

FIGURE 3: OVERVIEW OF THE BATHYMETRYIC SURVEYS AT BANC DU FOUR. AREAS COVERED BY THE 2010 SURVEY ARE OUTLINED BY BLACK SOLID LINES. AREAS COVERED BY THE 2011 SURVEY ARE OUTLINED BY DASHED BLACK LINES (FRANZETTI ET AL. 2013).

3.3 OBSERVED RAINFALL DATA, ID 27-37-42

The available rain measurements correspond to users/data providers with two slightly different perspectives: experts in charge of monitoring rain up to the regional level being part of the national monitoring network, and experts working for the municipality of Genova. Each of those two authorities operate their own network of rain gauges whose technical specification and spatial distribution matches the needs of their specific role in civil protection, in particular:

- Dataset ID 27&42: ARPAL professional network, 145 stations, measures every 5-20 minutes, GPRS and radio link connection, data size: 25 MB per day, coverage Regione Liguria (see Figure 4); in particular, dataset ID27 refers to measurements taken on November 4, 2011, while dataset ID42 concerns the rain measurements of September 29, 2013.
- Dataset ID 37: Genova Municipality, 30 stations, measuring every 3 minutes, GPRS or LAN connections, data size: 2MB per day, coverage Genova municipality. The available data are for September 29, 2013.

All data sets have been provided as collections of text files. Therefore, in order to test service 45 in the context of rainfall data, we converted part of the collected data to GeoTIFF files. In particular, by merging together two portions of datasets ID37 and ID42, we obtained a collection of 47 GeoTIFF files, each one capturing 30 minutes of data measurements over the whole

Regione Liguria, from 00.30 of September 29, 2013 to 00.00 of September 30, 2013. Figure 5 shows some examples of the aforementioned GeoTIFF files.

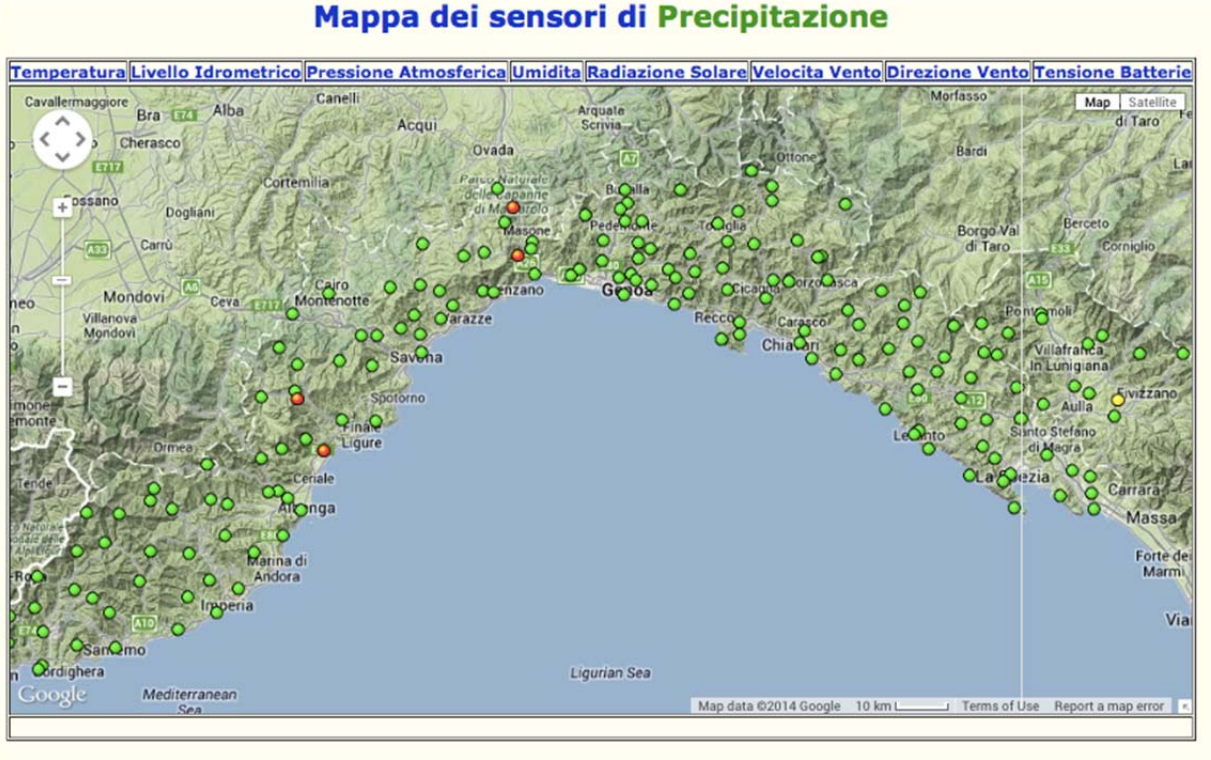

FIGURE 4: DISTRIBUTION OF THE RAIN GAUGES OF THE ARPAL/REGIONE LIGURIA

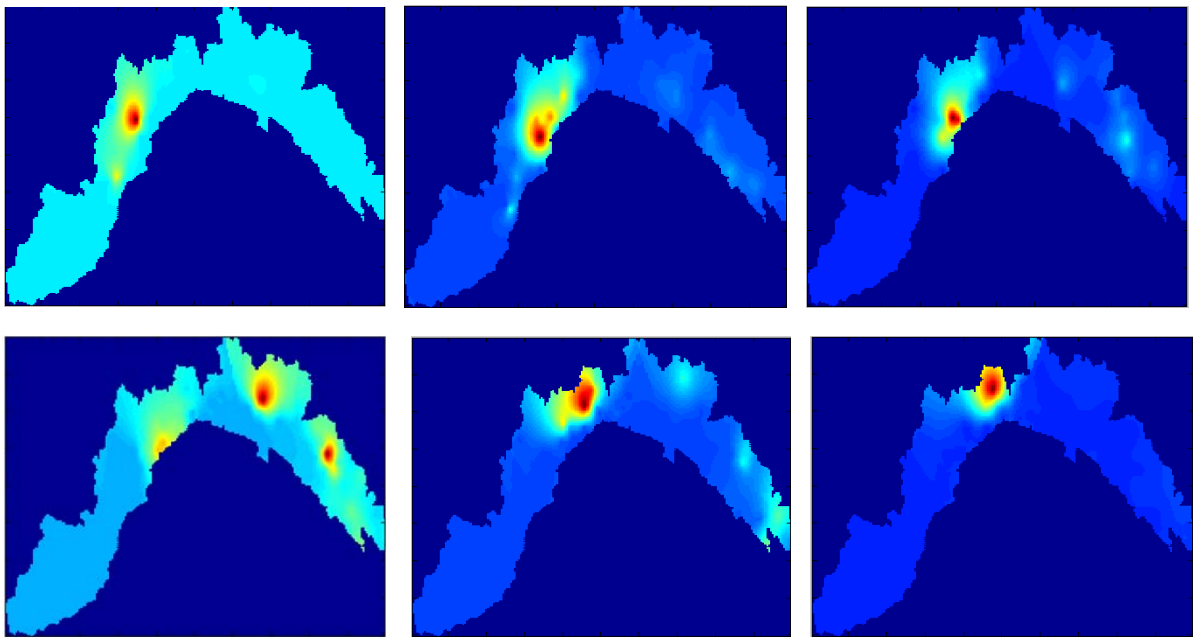

FIGURE 5: FROM TOP LEFT TO BOTTOM RIGHT, EVOLUTION OF THE 30-MINUTES CUMULATED RAIN MAP (COLOR CODED FROM BLUE TO RED), FROM 1.00 A.M TO 3.30 A.M OF SEPTEMBER 29 .

3.4 LOW RESOLUTION DIGITAL ELEVATION MODEL, ID 36

This data set is a collection of digital elevation models in GeoTIFF format and provides complete coverage of the Liguria region. Each DEM comes with a resolution of 5m. Even if the data set has not been associated so far with time-varying measurements, it has been used for functional testing due to the variability in size of the collected data, ranging from 12MB to 330 MB.

Table 4 and Figure 6 provide details about some samples from the dataset.

TABLE 4: DETAILS ABOUT SOME SAMPLES FROM DTASET ID 36

Type	Name	Resolution	Total Area	Size	ID
DEM	aveto	5m (xy) and 1m (z)	~150 km^2	12MB	36
DEM	la_spezia	5m (xy) and 1m (z)	~640 km^2	51MB	36
DEM	imperiese	5m (xy) and 1m (z)	~800 km^2	64MB	36
DEM	savonese	5m (xy) and 1m (z)	~1450 km^2	114MB	36

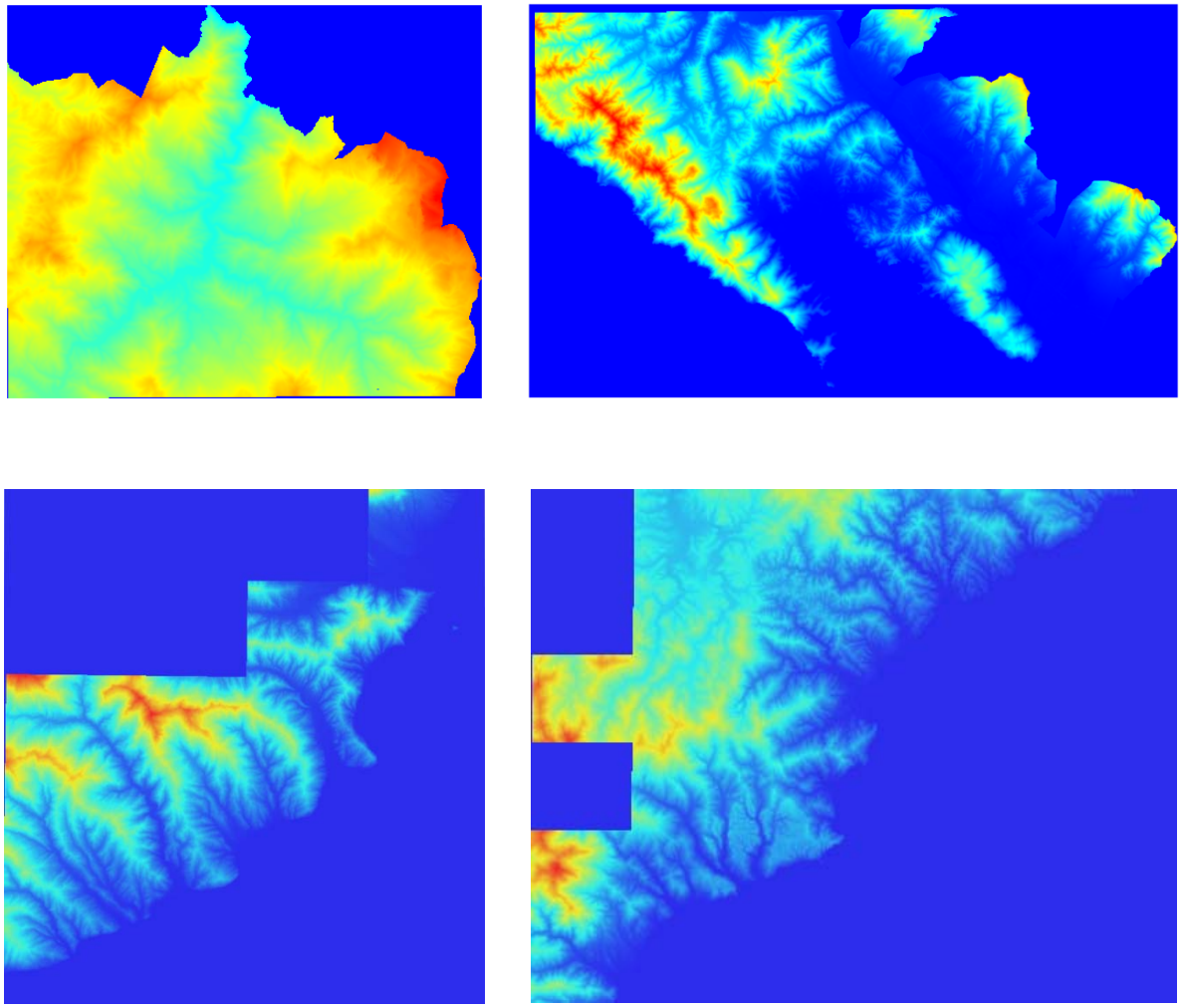

FIGURE 6: SOME DEM SAMPLES FROM DATASET ID 36: AVETO (TOP LEFT), LA SPEZIA (TOP RIGHT), IMPERIESE (BOTTOM LEFT) AND SAVONESE (BOTTOM RIGHT).

4 SERVICES

This section describes in detail the services developed in Task 4.5 and their experimental evaluation on the abovementioned sample data sets.

4.1 STOCHASTIC CHANGE DETECTION

This service evaluates if grid point wise differences are so large that a change is likely, given the variance of the input data. Two GeoTIFF format digital surface models with the same support (extent and resolution) are provided to the system as input for stochastic change detection. Cells with NaN in the input data are ignored and will yield corresponding NaN cells in the output data. Currently, the service can handle GeoTIFF 8-bit files directly, and converts 16-bit and 32-bit inputs internally with minor losses of precision. As input parameters, the user provides the level of significance **α**, and variances of the input data. As output, the system generates a GeoTIFF file, where for each grid point two attributes are determined, a 0/1 binary value indicating stability vs. change and a test statistic $\mathbf{T_q}$, which is the distance to model expressing stability in the VC-metric.
The service may require the support of three other services to obtain the required input:

1) Coarse registration (service #14)
2) Resampling (service #35)
3) Data intersection (service #12)

In the following lines, the mathematical calculation steps of the stochastic change detection algorithm are briefly explained. For each grid point two, say, height values and their variances are given$(h_1, {\sigma_{h1}}^2)$ and $(h_2, {\sigma_{h2}}^2)$:

1) Calculate the variance-covariance matrix of the observations

$$\mathrm{Q_{yy}} = \begin{bmatrix} {\sigma_{h1}}^2 & 0 \\ 0 & {\sigma_{h2}}^2 \end{bmatrix}$$

2) Design the matrix

$$A = [1 \quad 1]^T$$

3) Calculate the common height

$$y = (A^T * {Q_{yy}}^{-1} * A)^{-1} * A^T * {Q_{yy}}^{-1} * [h_1 \quad h_2]^T$$

5) Compute the vector of residuals

$$e = [h_1 \quad h_2]^T - [\mathrm{y} \quad \mathrm{y}]^T$$

6) Calculate the test statistic

$$T_q = e^T * {Q_{yy}}^{-1} * e$$

7) Evaluate T_q against critical value κ_α
Here the critical value κ_α is defined as the solution of the equation

$$\alpha = 1 - \mathrm{cdf}(\chi^2(\mathrm{q}, 0), \mathrm{x}), \qquad \text{with } \mathrm{q} = 1$$

The term $\chi^2(\mathrm{q}, 0)$ denotes the central Chi squared distribution with q degrees of freedom.
The algorithm is being developed for the operating systems Windows 7, 64-bit and Linux.
The amount of change, i.e. the test statistic T_q, will be displayed in a new window in 2D format with an appropriate color scale.

4.1.1 Quality

Accuracy: The accuracy of the change detection method depends on several different factors. The first factor is the conversion of the 3D point cloud into a gridded GeoTIFF image. In this stage the accuracy might be reduced due to residuals of the interpolation. If there are missing values in the generated gridded image, the user might prefer to apply an interpolation process before running the stochastic change detection algorithm. In this case, further artifacts might be introduced in interpolated areas. Finally, if the two input data sets are acquired with different sensors or under different acquisition conditions the ground sampling resolution and noise level might be different and deviate from the assumption that errors follow the same statistical distribution. Although the stochastic change detection algorithm takes the noise level of the input data sets explicitly into account, higher noise will still reduce the accuracy of the computation results.

Robustness: For now the designed service works well for 8-bit, 16-bit and 32-bit tiled/untiled signed/unsigned input GeoTIFF images. This large input image reading spectrum increases the robustness of the service and allows running the algorithm on all the test input examples. Warning messages and the comment prompt information texts provide guidance for the user and signal possible problems.

4.1.2 Scalability

The complexity of the system can be assumed as a linear function O(n). A computation time of a couple of seconds is expected for input data sets where each image contains 1000x1000 grid points. Further development will address the exploitation of the sparseness of the matrix Q_{yy} and the use of the MapReduce framework for efficient processing of large raster datasets.

4.1.3 Degree of human intervention

If the input images are not registered, we expect the user to use previously developed services in order to find the intersection region of the two input images and register this intersection part on each other. If the user wants to fill non-value pixels of the data, then an interpolation service must be called to generate an interpolated image where all pixel values have real values. After preparing the input data, the stochastic change detection algorithm can be called to estimate changes and their degrees. We expect the user to enter the standard deviation of each input image. Otherwise it will be calculated automatically. Using test data, the test statistics will be calculated automatically and this data will show the degree of changes as gray values. Using the "level of significance (α)" the critical value will be analyzed as either "accepted" or "rejected". So in this way, we obtain a second output image which is a binary map showing two classes as changed and unchanged areas. We expect the user to enter the level of significance value. Otherwise the default value 0.05will be used.

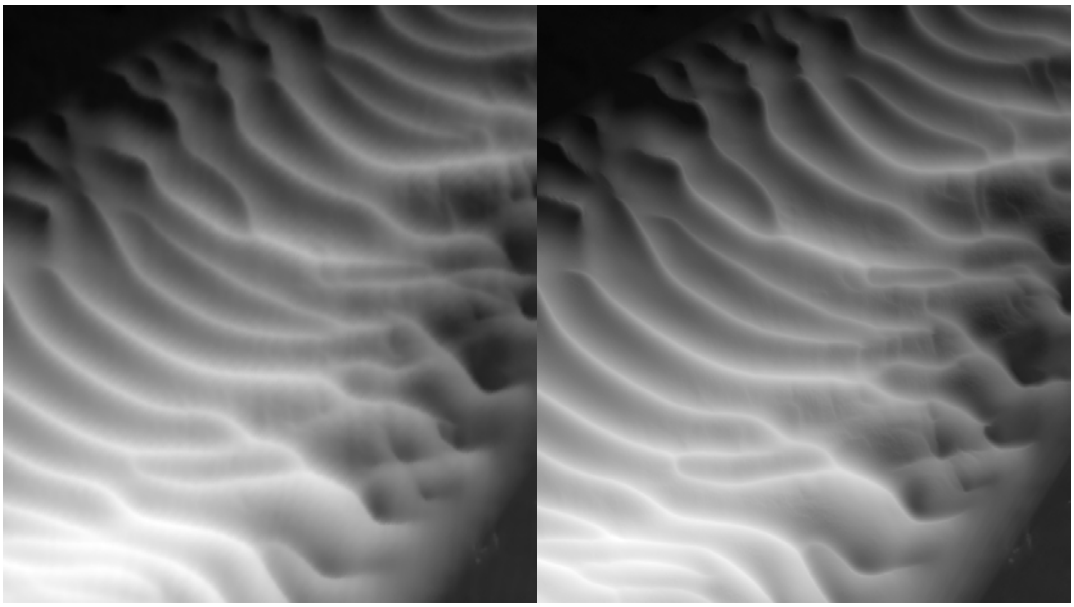

(A) (B)

FIGURE 7: FOR TESTING THE STOCHASTIC CHANGE DETECTION ALGORITHM WE HAVE CHOSEN TWO BATHYMETRY DATA ACQUIRED OFFSHORE THE COAST OF BRITTANY. CHANGES IN THE SEA FLOOR DUE TO DUNE MIGRATION CAN BE DERIVED FROM THOSE IMAGES. (A) THE BATHYMETRIC MODEL FOR 2009 AND (B) FOR 2011.

In Figure 7, two GeoTIFF images of the seafloor topography in near-coastal waters in Brittany are displayed. The input images (A) and (B) depict the seafloor on two different dates (2009 and 2011, respectively). They are co-registered and share the same resolution and extent. The objective of the analysis is to detect vertical sea bottom layer change using the developed stochastic change detection algorithm.

The test statistics computed during the stochastic change detection analysis are displayed in Figure 8. Here high values correspond to higher vertical changes. The test statistics are given as a degree of change in terms of numbers relative to each other which always have a positive value but do not have a unit.

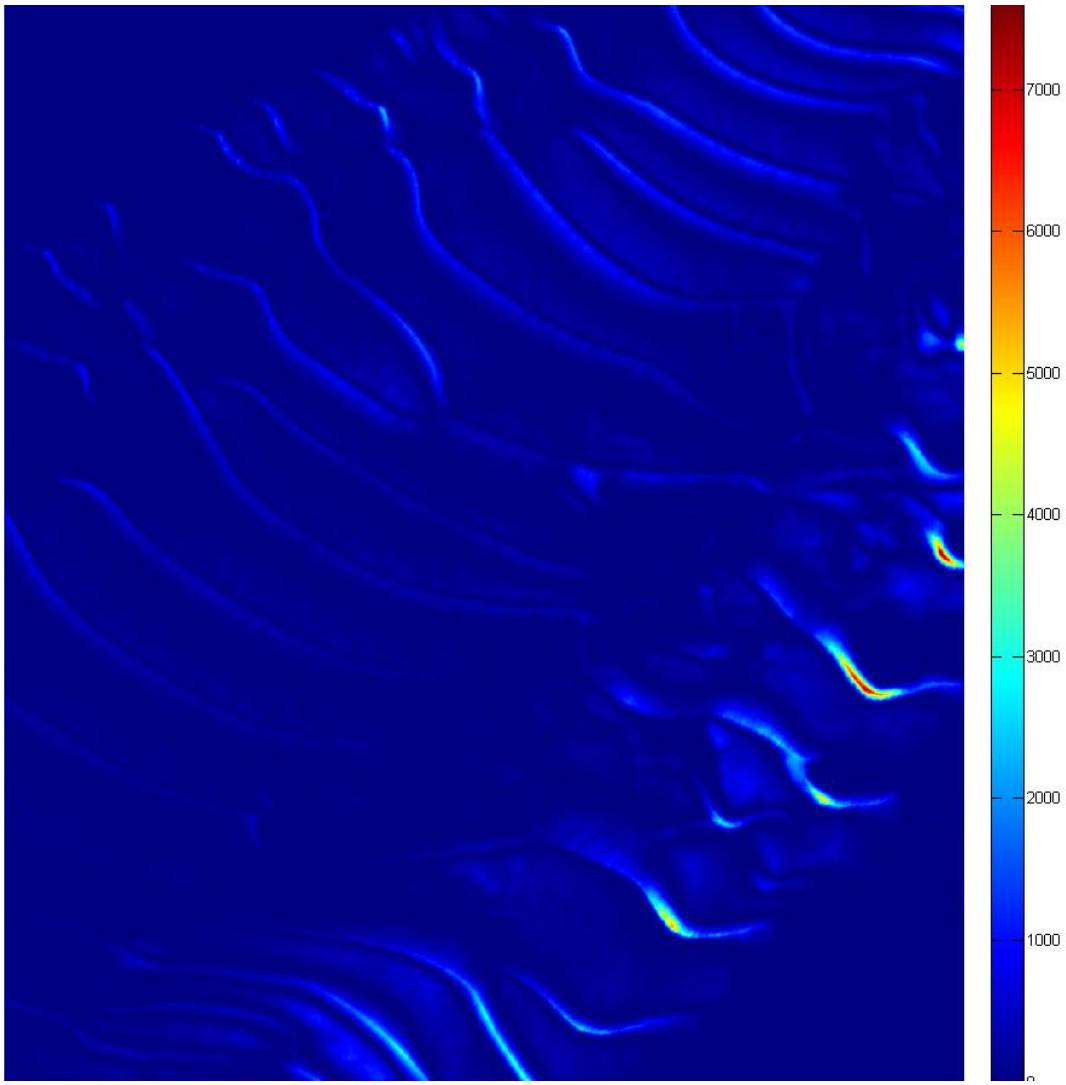

FIGURE 8: RESULTS OF THE STOCHASTIC CHANGE DETECTION ANALYSIS TEST STATISTICS.

Figure 9 shows the pixels which are accepted as a significant change according to the comparison with the upper critical value. The change image clearly depicts the pattern of the dune migration.

FIGURE 9: DETECTED CHANGES

4.2 TOPOLOGICAL CHANGE DETECTION

This service for change detection is based on a topological analysis of the distance map obtained from two co-registered gridded point-clouds (GeoTIFF) in order to find pairwise corresponding maxima, minima and saddles. Changes in the spatial location of maxima, minima and saddles are considered as topological events. An adaptation of the service to triangulations (.ply) is currently under development.

The service is inspired by *topological persistence* (Edelsbrunner and Harer 2010), a theoretical framework rooted in algebraic topology, which recently has been revealed as a viable option for the analysis of data, with applications ranging from shape analysis and comparison (Carlsson et al. 2005; Chazal et al. 2009), to data simplification (Bauer et al. To appear; Bauer et al. 2012) and reconstruction (Zheng et al. 2011). This is due to properties like topological consistency when analysing data, quantifiable robustness in the presence of noise, and a mathematically sound metric for assessing data variations.

Given two co-registered gridded point clouds sharing a region X, the distance map $f: X \to \mathbb{R}$ is obtained as the difference between the corresponding height functions (z-values; for symmetry reasons, we consider the absolute value of the distance map). Using this, a *filtration of* X is computed by considering the sequence of sublevel sets $X_u = \{x \in X \mid f(x) \leq u\}, u \in \mathbb{R}$, nested by inclusion. Along the filtration, two different types of topological changes are tracked: the birth of new connected components and the death (that is, the merging with other connected components) of existing ones. Topological events are encoded by properly pairing the maxima, minima and saddle values of the function f, and possibly ranked by importance: The greater the persistence (that is, the difference between the function's values representing the birth and the death of a connected component), the more important the topological event associated to that component.

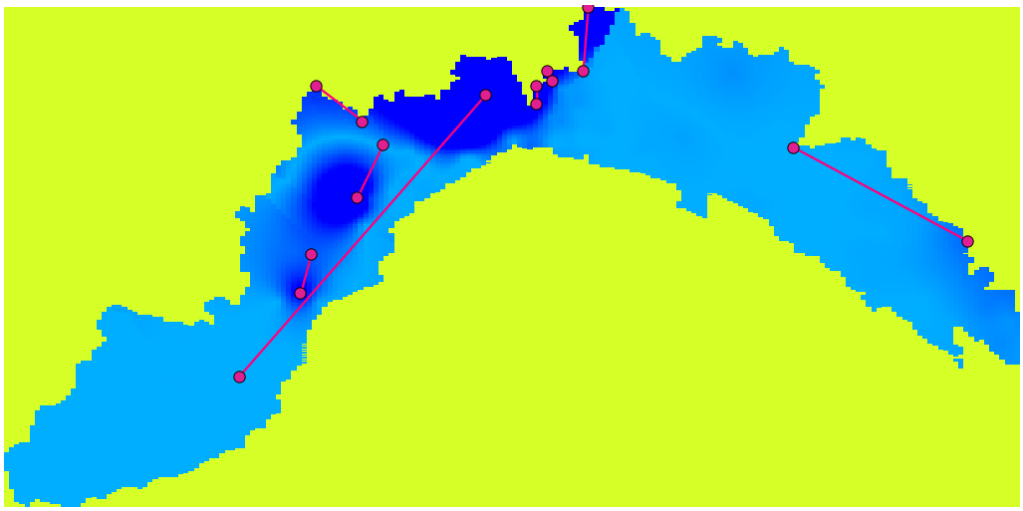

(a)

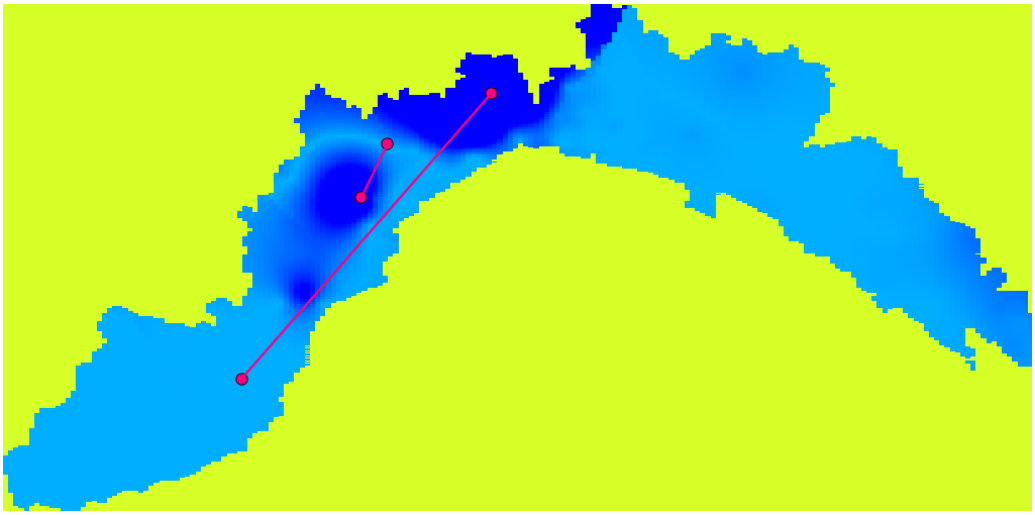

(b)

FIGURE 10: TWO EXAMPLES OF TOPOLOGICAL CHANGE DETECTIONS WITH RESPECT TO LOWER (A) AND HIGHER (B) INPUT THRESHOLDS. DATASET: GEOTIFF FILES OBTAINED FROM THE OBSERVED RAINFALL DATA DATASETS, ID 27-37.

In practice, the algorithm extracts a list of critical points (maxima, minima and saddles) properly paired and representing the occurrence of topological events. The corresponding list of paired critical values allows for ranking topological events by importance, and possibly prunes them

according to an input threshold. Figure 10 shows two examples of the algorithm in action for two different input thresholds.

In both the examples, the input region X is the whole Liguria region (the bluish part in both pictures). The distance map $f: X \to \mathbb{R}$ is defined as $f(x) = -||f_1(x) - f_2(x)||$ for all $x \in X$, with f_1 and f_2 representing two of the rain maps described in Section 3.3 and depicted in Figure 5. The map f is color-coded from dark blue to light blue: dark blue areas correspond with the lowest values for f, which in turn reveal the largest differences between f_1 and f_2. As for Figure 10a, a number of points are paired together (arcs are depicted to highlight pairings): Each pair is composed by a saddle/maximum point and a minimum point for the function f, and can be associated to the presence of a "bump" in the function f. Here the paradigm is that the bigger the bump (and hence the larger the difference between the values of f in the associated pair), the greater the difference between f_1 and f_2 in that part of the region X.

In Figure 10b, a different choice for the input threshold allows us to consider only the largest changes in the same distance map, thus disregarding details and possibly noise. An example of a similar analysis, but on different data input, is displayed in Figure 11.

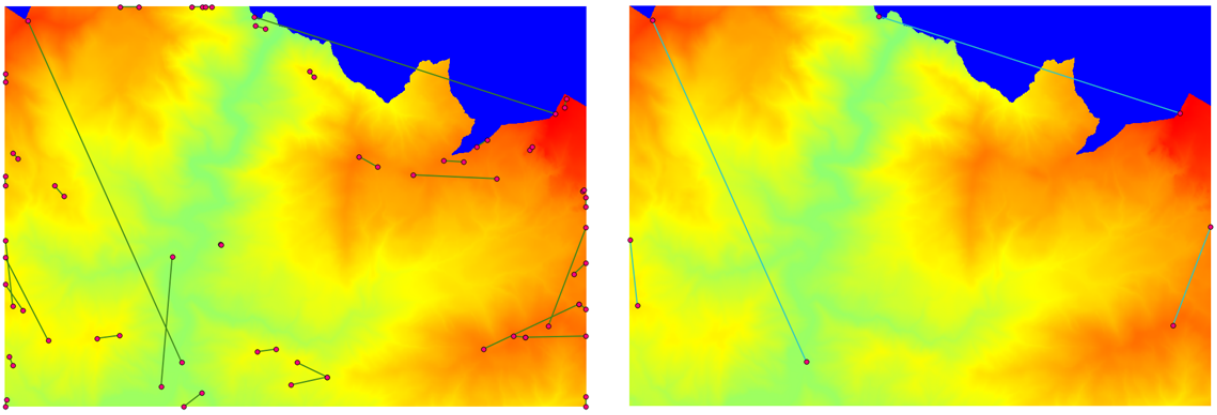

(a) (b)

FIGURE 11 TWO EXAMPLES OT TOPOLOGICAL CHANGE DETECTION WITH RESPECT TO LOWER (A) AND HIGHER (B) INPUT THRESHOLDS.. DATASET: GEOTIFF IMAGE REPRESENTING PART OF VAL D'AVETO (REGION LIGURIA DATASET, ID 36)

The service currently runs on gridded point clouds (GeoTIFF), but will be extended to run on triangulations (.ply). An optional parameter is the input threshold, namely the *persistence threshold*, which allows for pruning all the topological events associated with lower persistence. The output is threefold:

- List of topological changes/events in terms of the distance map's values (*persistence diagrams*, .mat 2D array);
- Total persistence (scalar value given by the persistence sum of all topological events, providing an overall measure of the magnitude of topological changes);
- List of 2D points, properly paired, at which topological changes occur (points and arcs shape files).

The service is implemented in C/C++ and has dependencies on libraries for dealing with GeoTIFF and shape files, namely SHAPELIB, GeoTIFF and LibTIFF. It is compiled under Windows and it is planned to work on Windows and Linux OS.

Visualization: If required, visualization of the distance map, in the form of a GeoTIFF file; visualization of points at which topological changes occur, in the form of shapefiles, up to the chosen persistence threshold.

4.2.1 Quality

Accuracy: Topological changes are detected at the same level of the machine precision used to store the values of the distance map.

Robustness: The algorithm is robust to perturbation of the distance map: theoretical results show that small changes in the considered distance maps imply only small changes in the persistence of topological events (possibly small persistence events may disappear).

4.2.2 Scalability

In order to detect topological changes for gridded point clouds (GeoTIFF), the algorithm takes $O(n\alpha(n))$ operations, with n the number of points in the input gridded point cloud, and α the inverse of the Ackermann function. Moreover, recent results (Bauer et al. 2013), (Lipsky et al. 2011), (Lewis and Zomorodian 2012) show the possibility of introducing a distributed computation of persistence, which will be objects of further study for the next versions of the service.

4.2.3 Degree of human intervention

One parameter a user has to choose is the persistence threshold τ, in the form of a scalar value ranging from 0 to 1. According to the threshold, the algorithm will give as output all pairings (for $\tau = 0$) or only the pairings having persistence greater than $\tau \cdot (max_X f - min_x f)$. A second parameter is given by NoDataValue, that is, the value which is used in the GeoTIFF input to indicate parts of the data that do not have to be considered.

4.3 2D DISPLACEMENT MEASUREMENTS USING DSM/DTM/DEM AND OPTICAL IMAGES

This service provides tools for measuring piece-wise locally the shift among two or more co-registered datasets provided in GeoTIFF format. The service has been furnished based on the MicMac library focusing in particular on measurements among very-high resolution optical images and digital elevation models. To assess the performance and guide further development the service has been compared against state-of-the art image matching methods in terms of quality of the results, scalability of the computation and the required amount of user interaction. In addition to the matching algorithm a set of tools for the visualization of the derived displacement fields have been developed.

4.3.1 Quality

The quality of the displacement measurements can be assessed considering three main aspects being (a) robustness against false positive matches in the presence of noise such as vegetation and rugged topography, (b) robustness against decorrelation in the presence of strong surface changes and (c) the absolute accuracy of the derived measurements. With only limited ground truth available we focus here on the two first aspects.

Major sources of false positive matches are vegetation and shadows which, however, can easily be identified through an analysis of the input images and a DEM. Service 60 therefore comprises tools to generate a vegetation/shadow mask based on the input images combined with a digital elevation model. The masking routine as well functions to visualize the derived displacement fields have been implemented as R functions and can be interfaced through a few simple calls. The following example illustrates how the functions can be used to significantly reduce the amount of false matches and visualize the results.

Workflow to clean up displacement fields

Load parameter file that was used for the correlation

```
file <- "/data/ParamSat.xml"
```

Visualize raw displacement field

```
DisVisMM (file, max.displacement = 5, thresh.correl=0.1, scale.arrows=30,
background="image",title="Super Sauze, 07 Aug -05 Oct, MICMAC")
```

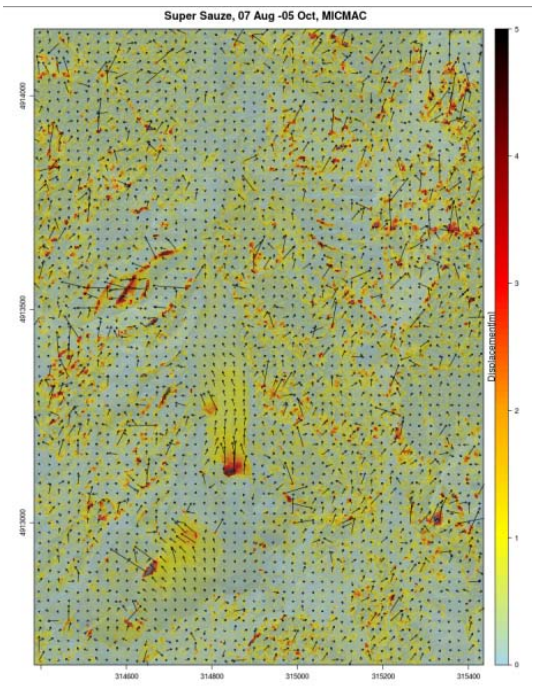

Load input images and DEM

```
MS <-  "/data/orthoimg_phr1a_ms_20120807_supersauze.tif"
PAN <- "/data/orthoimg_phr1a_p_20121005_01_supersauze.tif"
DEM <-  "/data/dsm_supersauze.img"
```

Automatically generate mask and visualize

```
image.mask <- create.ImageMask(MS, PAN)
plot(image.mask)
```

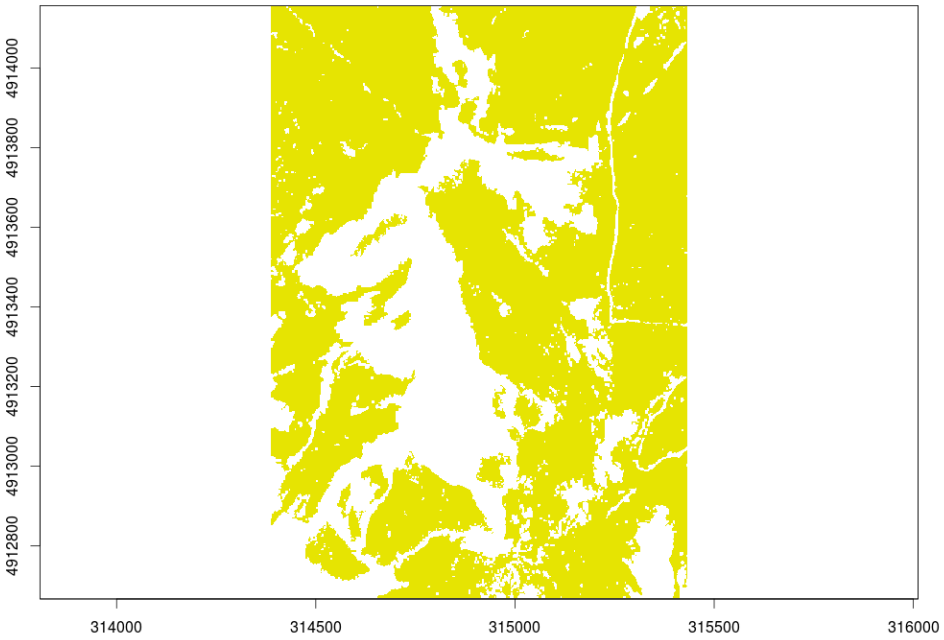

Apply mask and directional filter and visualize the result

```
DisVisMM (file, image.mask, DEM, max.displacement = 5, thresh.correl=0.1,
scale.arrows=30, background="image",title="Super Sauze, 07 Aug -05 Oct, MICMAC")
```

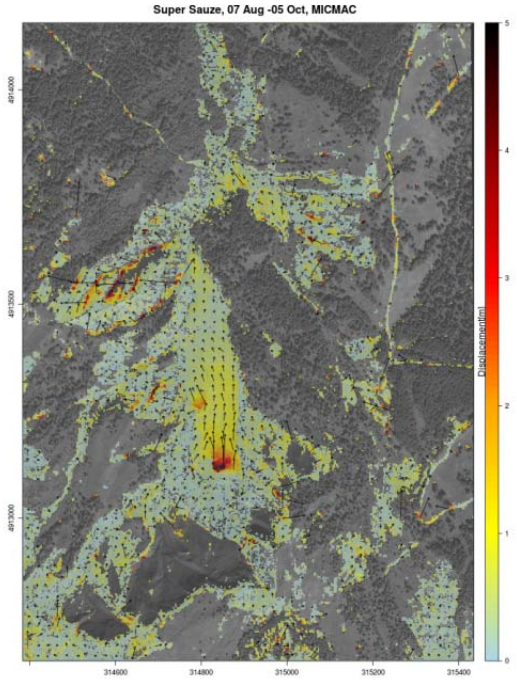

Figure 12 shows a first comparison of the furnished service for 2D displacement measurements against state-of-the-art methods currently most commonly used for such applications. While the general pattern of the derived fields is similar, it can be noted that MicMac provides an overall smoother flow field which must be attributed to the spatial regularization implemented in the algorithm.

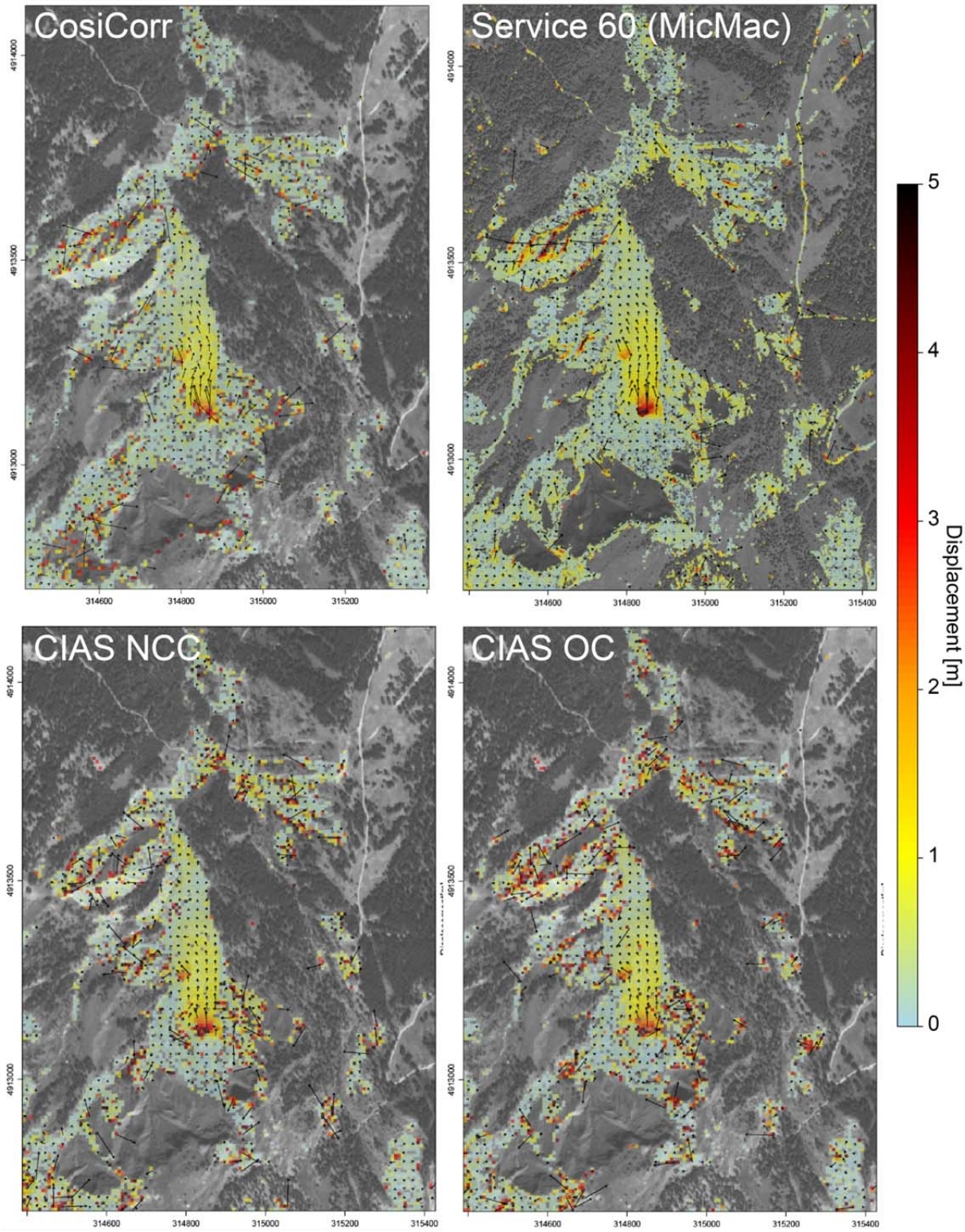

FIGURE 12: DISPLACEMENT FIELD OF THE SUPER SAUZE LANDSLIDE DERIVED FROM ORTHOIMAGES (AUG 2012 – OCT 2012) USING DIFFERENT IMAGE MATCHING TECHNIQUES.

Outliers outside the landslide (central part of the image) are generally more prominent with CIAS and in particular when the orientation correlation (OC) is used. MicMac yields slightly more false matches than CosiCorr which must be attributed to a relative conservative threshold on the correlation coefficient. Among all tested algorithms MicMac was the only method that provided correct measurements for the areas with the highest displacement rates of around 5m. Furthermore, the service enables parallel execution and allows measurements at full resolution, which was not tractable with the serial implementations of the competing methods. Consequently, the derived displacement field has a resolution that is 16 times higher than with CIAS and 4 times higher than with CosiCorr and therefore better depicts local variations of the non-rigid displacement.

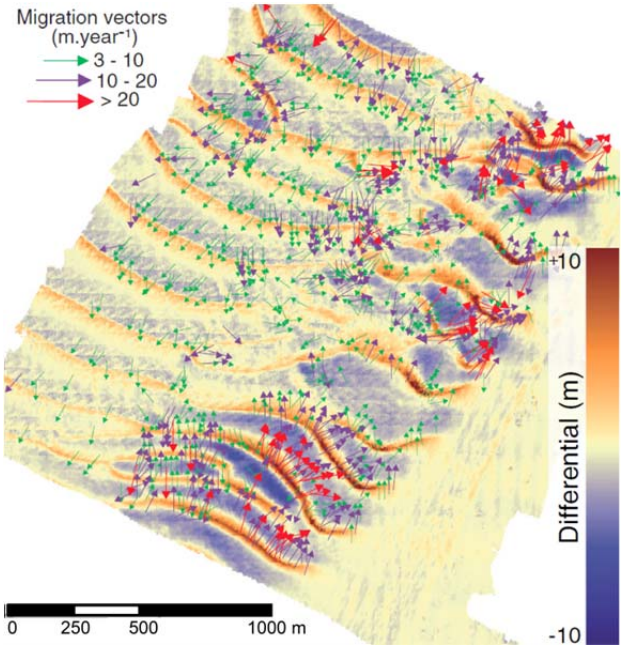

FIGURE 13: MOTION FIELD FOR A SUBSET OF THE BANC DE FOUR DERIVED WITH THE CNES CORRELATOR (VADON AND MASSONNET 2000). MODIFIED AFTER (FRANZETTI ET AL. 2013).

A series of further experiments was dedicated to the comparison of the performance of the different matching techniques for motion measurements of submarine dunes. Figure 13 illustrates results that were obtained previously using a correlation technique following (Vadon and Massonnet 2000) and that were considered as a benchmark for further improvements.

The experimental assessment focused on a correlation of two surveys carried out at the Banc de Four (offshore south-west Britany) in 2009 and 2010, respectively. Figure 14 illustrates that the MicMac correlator provided within service 60 provides a displacement field that is consistent with the results from previous studies (compare Figure 13 and the north-east section in Figure 14) but spatially more consistent and denser. Though in-situ measurements that would allow quantifying the absolute accuracy of the different matching techniques are generally lacking in a sub-marine setting, Figure 14 illustrates that service 60 outperforms competing methods in terms of completeness and noise level. It was attempted to optimize the parameters for CosiCorr and CIAS (e.g., correlation window sizes for the presented results were comparatively large) in a trial-error procedure but we were not able to obtain measurements with a satisfactory coverage and interpretability.

Service 60 provided a motion field that is consistent with the expectations when considering the asymmetry of the dune morphology (Figure 15). Some false matches are related to areas with relatively low texture and significant noise within the bathymetric measurements. Such issues remain to be addressed during future developments of the toolbox.

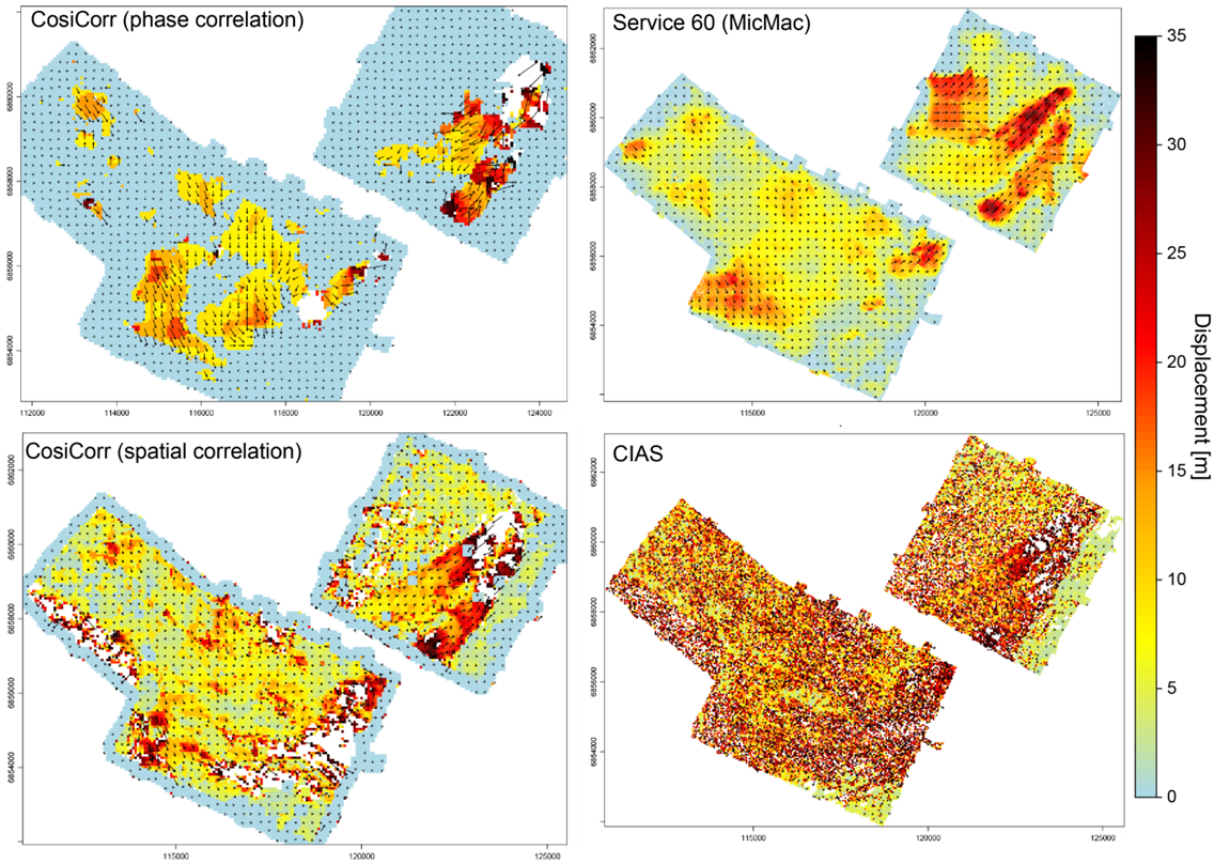

FIGURE 14: DISPLACEMENT FIELDS DERIVED FROM THE BATHYMETRIC DATA SET BANC DE FOUR 2009-2010 USING DIFFERENT MATCHING ALGOIRTHMS

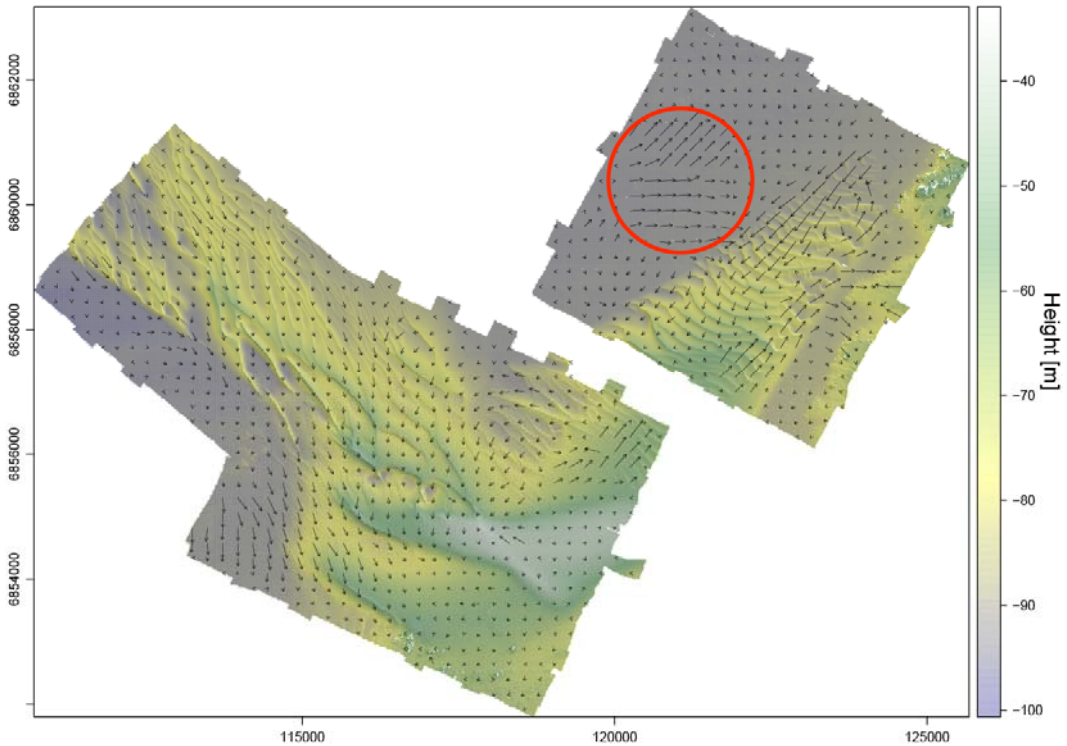

FIGURE 15: RESULTS OF SERVICE 60 ON THE BATHYMETRIC DATA AT BANC DE FOUR (SAME AS IN FIGURE 14) VISUALIZED WITH THE FUNCTION DEVELOPED WITHIN THE 4.5.1 TOOLKIT. THE RED CIRCLE MARKS FALSE MATCHES RESULTING FROM LOW TEXTURE AND NOISE IN THE BATHYMETRIC DATA.

4.3.2 Scalability

For most applications (e.g., landslide deformation, dune migration, glacier flow) the measurement of displacement rates with image correlation techniques is currently not time critical since in most cases data archives with a temporal frequency not below several months are analysed. With an increasing fleet of high and very high resolution optical satellites, however, the acquisition interval approaches a few days (e.g., Pléiades, Sentinel-2) and near-real-time monitoring is therefore likely to become a more prominent issue in the near future.

To assess the runtime and the computational complexity of all tested algorithms an experiment was set up using the VHR satellite image presented in Figure 12 measuring 2099 by 2978 pixel. We ran each image matching technique several times on the full resolution image and successively subsampled versions and recorded the execution time. While all tests were performed on an 8 threads Intel i7-4800MQ with 2.7 GHz, only MicMac enables parallel processing and CIAS and CosiCorr run on one core only. The results shown in Figure 16 show that the execution times for all three methods increase linearly corresponding to an O(n) time complexity whereas the slope of the runtime increase differs significantly. In particular CIAS shows a very steep increase in the runtime, rendering for example batch processing of several full scene images intractable. CosiCorr provides an intermediate runtime whereas MicMac clearly outperforms the CIAS and CosiCorr in terms of execution time. To put those figures in a practical context we note that an entire Pléiades scene (20x20 km) measures 40000 by 40000 pixels and modern high-resolution satellites such as SPOT 5 and SENTINEL-2 measure 10000 by 10000 pixels. The matching of an entire Pléaides scene would thus take approximately 6 days on our test machine. The parallelization in MicMac is handled with GNU MAKE and we will investigate its implementation on the IQmulus Cloud for the next version of the Task 4.5 toolkit. All three algorithms internally use tiling and hence no memory limitations where encountered or should be expected for larger images.

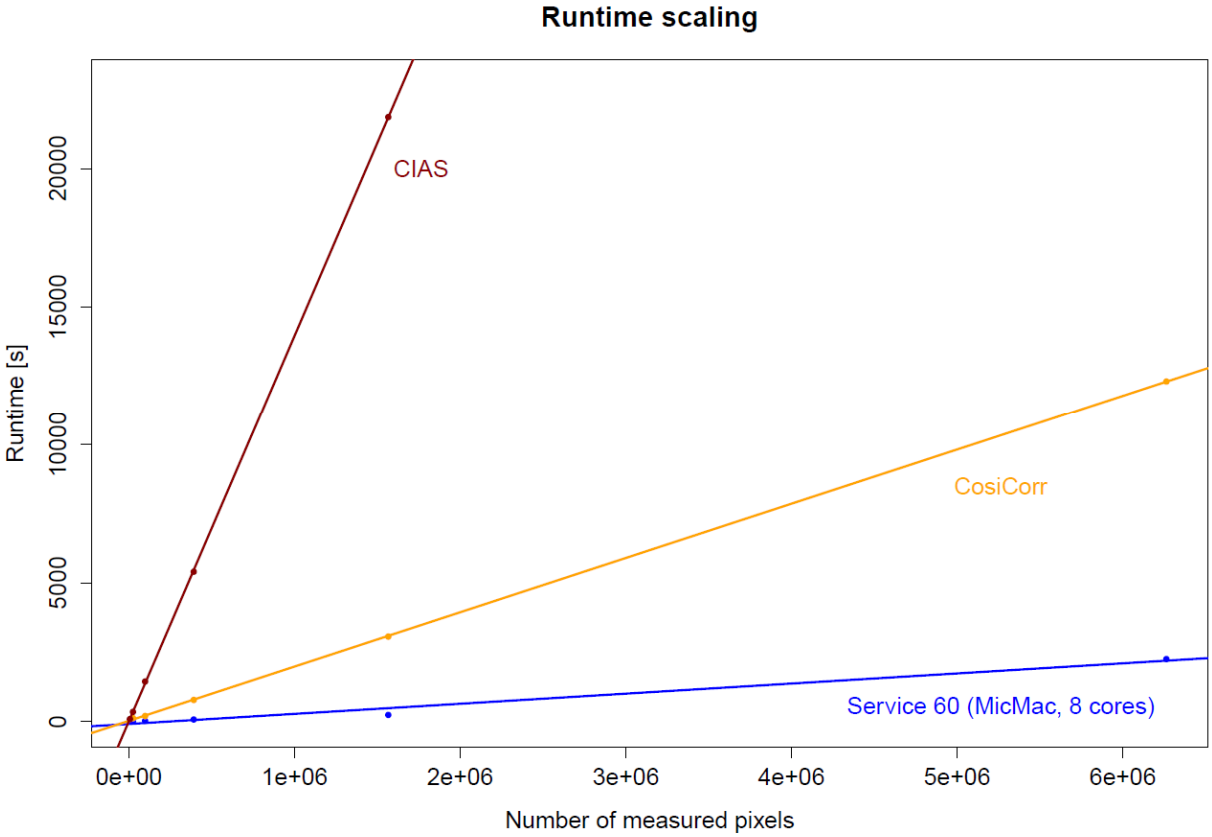

FIGURE 16: RUNTIME VERSUS NUMBER OF MEASURED PIXELS FOR CIAS, COSICORR AND MICMAC.

4.3.3 Degree of Human Intervention

The image matching algorithm used for service 60 has several parameters that can be adjusted by the user for specific applications and have a direct impact on the obtained displacement fields. All parameters can/have to be specified in an XML file that is read out at runtime and controls the matching process. A commented XML template given in section 4.3.3.1 shows all adjustable parameters. While some of the parameters generally need no adjustment (e.g., number of explored directions for the spatial regularization), other parameters are application specific and should be accessible to the expert users. In this context three different levels of user interaction could be envisaged.

Expert user
The full set of parameters is exposed to the user. Default values and guidance on the settings are provided.

Advanced user
Among all parameters we identified five that must be considered as relatively sensitive and application specific. This concerns the size of the search area, the size of the correlation window, the strength of the regularization, the resolution level and the correlation threshold.

Zoom factor [DeZoom]: The algorithm follows a hierarchical scheme and allows determining a subpixel shift at different resolutions where a zoom factor of 1 corresponds to the full resolution, 2 corresponds to half the original resolution, 4 corresponds to ¼ of the original resolution and so forth. While results at lower resolutions are generally less precise, the computation is significantly faster and allows obtaining quickly a first order approximation of the displacement (Figure 17b).

Size of the search area [Inc]: The value is expressed in pixels and constrains the search space in the first iteration. It should be set equal to or larger than the maximum expected displacement. Smaller search areas reduce the computational load and theoretically reduce the risk of false matches in the first iteration.

Regularization [RegulBase]: This parameter controls the strength of the spatial regularization. An increased value generally promotes a smoother displacement field that appears less noisy but may also smooth out smaller local variations (Figure 17c).

Window size [SzW] and correlation threshold [CorrelMin]: Those two parameters are interrelated since a larger window size generally leads to on average higher correlation coefficients. Strong local deformation counteracts this affect and a smaller window size (10x10) might be more appropriate when the local deformation is strong. Larger window sizes generally lead to more homogeneous displacement fields. This is also true for a high correlation threshold (e.g. CorrelMin > 0.8) since many measurements with a low NNC are ignored and the displacement vectors then depend on the measurements within neighbouring cells (Figure 17d).

Standard user
For users not familiar with algorithmic details two standard XML files have been created where one is optimized for displacement measurements from VHR satellite images and the other is optimized to measure dune migration from interpolated bathymetric data (Figure 17a). In the standard case the user thus only has to choose among those two use cases and provides an estimate of the maximum expected displacement expressed in number of pixels.

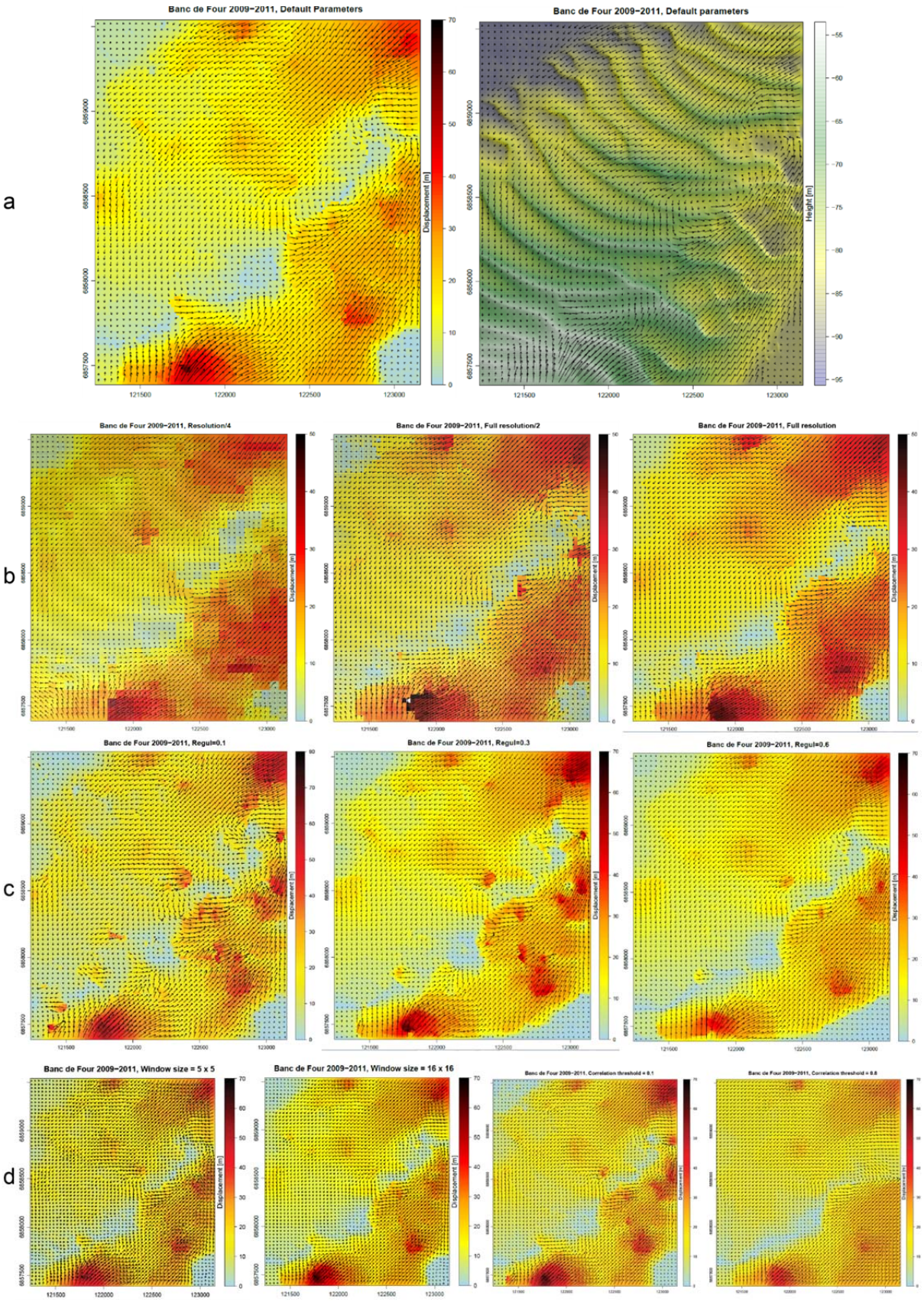

FIGURE 17: EXAMPLARY RESULTS ILLUSTRATING THE INFLUENCE OF THE MAIN ALGORITHM PARAMETERS. (A) RESULTS WITH THE DEFAULT PARAMETERS OPTIMIZED FOR MEASURING DUNE MIGRATION, (B) RESULTS AT DIFFERENT RESOLUTIONS, (C) RESULTS WITH DIFFERENT REGULARIZATION, AND (D) RESULTS DEPENDENT OF WINDOW SIZE AND CORRELATION THRESHOLD.

4.3.3.1 A Pattern file for using MicMac for measuring the migration of submarine sand-dunes

```
<ParamMICMAC>
    <DicoLoc>

<!--  Define input, TIFs with the same resolution are mandatory-->
         <Symb> Im1=four_bathy_RGF93_2m.tif  </Symb>
         <Symb> Im2=2011_noNA.tif </Symb>
         <Symb> Masq=four_bathy_RGF93_2m_Mask </Symb>

         <Symb> Dir=MEC/</Symb>              <!-- output folder -->
         <Symb> Pyr=Pyram/</Symb>            <!-- sub folder for image pyramids folder -->
         <Symb> Inc=20.0  </Symb>            <!-- search range in pixel -->
         <Symb> Pas=0.2 </Symb>              <!-- default step size for matching -->
         <Symb> Teta0=0 </Symb>              <!-- optional directional regularization angle -->
         <Symb> UseMasq=true </Symb> <!-- optional use of a mask -->
         <Symb> UseTeta=false </Symb>        <!-- optional use of directional regularization  -
->
         <Symb> RegulBase=0.3 </Symb>        <!-- default regularization parameter  -->
         <Symb> UseDequant=false </Symb>     <!--optional interpolation, not used -->

          <Symb>  SzW=4 </Symb>                    <!-- search window size [-4,4]x[-4,4]-->


         <Symb> CorrelMin=0.5 </Symb>        <!-- measurements with an NCC below this threshold
are not considered -->
         <Symb> GammaCorrel=2 </Symb>        <!-- >1 to give higher weight to measurements with
high NCC  -->

         <Symb> PdsF=0.1 </Symb>
         <Symb> NbDir=7 </Symb> <!-- number of paths used in SGM-like regularization -->
         <eSymb> P0= / ${PdsF} +   ${PdsF} / 0 ${NbDir} </eSymb>
         <eSymb> P1= / ${PdsF} +   ${PdsF} / 1 ${NbDir} </eSymb>
         <eSymb> P2= / ${PdsF} +   ${PdsF} / 2 ${NbDir} </eSymb>
         <eSymb> P3= / ${PdsF} +   ${PdsF} / 3 ${NbDir} </eSymb>
         <eSymb> P4= / ${PdsF} +   ${PdsF} / 4 ${NbDir} </eSymb>
         <eSymb> P5= / ${PdsF} +   ${PdsF} / 5 ${NbDir} </eSymb>
         <eSymb> P6= / ${PdsF} +   ${PdsF} / 6 ${NbDir} </eSymb>
         <eSymb> P7= / ${PdsF} +   ${PdsF} / 7 ${NbDir} </eSymb>
         <Symb>
VPds=[${P0},${P1},${P2},${P3},${P4},${P5},${P6},${P7},${P6},${P7},${P4},${P3},${P2},${P1}]
</Symb>
         <eSymb> NbDirTot=* 2 ${NbDir} </eSymb>
         <eSymb> Regul=* ${RegulBase}  ? ${UseTeta} 3 1 </eSymb>
    </DicoLoc>
<!-- ************************************************************
Search space parameters
  ************************************************************-->
    <Section_Terrain>
      <IntervParalaxe>
        <!--Px1IncCalc and Px2IncCalc define the search space on the first level of
               the pyramid. By default the value of Inc is used.-->
        <Px1IncCalc>  ${Inc}  </Px1IncCalc>
        <Px2IncCalc>  ${Inc}   </Px2IncCalc>

        <!--Px1Moy and Px2Moy fixes the mean parallax value and thereby constrains
               the search region on the first level of the pyramid. The resulting displacement
values
               are    expressed relative to Px1Moy and Px2Moy. Probably only useful
               if both images have a systematic offset.-->
        <Px1Moy >  0.0     </Px1Moy>
        <Px2Moy >  0.0   </Px2Moy>

      </IntervParalaxe>

      <Planimetrie>
       <!-- Image mask used to constrain the processing existent for the correlation.
           The mask should have the same resolution and extent than the input image.
           If the file doesn't exist it will be created automatically considering the
           full image extent -->
        <#WHEN VTEST=${UseMasq}>
            <MasqueTerrain>
                <MT_Image> ${Masq}.tif </MT_Image>
```

```
                <MT_Xml>   ${Masq}.xml </MT_Xml>
            </MasqueTerrain>
        </#WHEN>
      </Planimetrie>
    </Section_Terrain>

 <!-- ************************************************************
Define matching geometry
    ************************************************************ -->
    <Section_PriseDeVue>
        <GeomImages> eGeomImage_Epip </GeomImages>
        <Images>
            <Im1> ${Im1} </Im1>
            <Im2> ${Im2} </Im2>
        </Images>
    </Section_PriseDeVue>

<!--  ************************************************************
Main parameters for the hierarchical matching. First iteration is for
initialization only and <DeZoom > -1 </DeZoom> is mandatory.
Successive iterations must have an equal or decreasing zoom factor.
e.g. 4,2,1,1
************************************************************ -->
    <Section_MEC>
        <ChantierFullImage1> true </ChantierFullImage1>

        <ClipMecIsProp> false </ClipMecIsProp>

        <EtapeMEC> <!-- First iteration for initialization -->
            <DeZoom > -1 </DeZoom>   <!-- -1 is mandatory -->
            <SzW> ${SzW}   </SzW>    <!-- window size-->

                      <!-- port values from the header of the XML-->
            <CorrelMin>  ${CorrelMin} </CorrelMin>
            <GammaCorrel>  ${GammaCorrel} </GammaCorrel>
            <DynamiqueCorrel> eCoeffGamma </DynamiqueCorrel>

                      <!-- parameters for saptial regularization with dynamic programming-->
            <AlgoRegul> eAlgo2PrgDyn </AlgoRegul>
            <ModulationProgDyn Portee="Globale">
                <EtapeProgDyn>
                    <ModeAgreg>    ePrgDAgrSomme   </ModeAgreg>
                    <#WHEN VTEST=${UseTeta}> <!-- optional directional-->
                        <Px1MultRegul> ${VPds} </Px1MultRegul>
                        <Px2MultRegul> ${VPds} </Px2MultRegul>
                    </#WHEN>
                    <NbDir>      ${NbDirTot}     </NbDir>
                    <Teta0>    ${Teta0}    </Teta0>
                </EtapeProgDyn>
                <Px1PenteMax > 2.0 </Px1PenteMax> <!-- max. parallax among neighbouring pixel
in x-->
                <Px2PenteMax > 2.0 </Px2PenteMax> <!-- max. parallax among neighbouring pixel
in y-->
            </ModulationProgDyn>
            <Px1Regul>  ${Regul}    </Px1Regul> <!-- porting regularization parameter-->
            <Px2Regul>  ${Regul}   </Px2Regul>  <!-- porting regularization parameter-->

            <GenImagesCorrel> true </GenImagesCorrel>

                      <!-- interpolation algorithm used for subpixel matching,
                      by default a sinc kernel with a support [-5,5]x[-5,5] -->
            <ModeInterpolation> eInterpolSinCard </ModeInterpolation>
            <SzSinCard>  5.0 </SzSinCard>
            <SzAppodSinCard>  5.0 </SzAppodSinCard>

                      <!-- search space tolerance relative to the parallax
                      determined in the previous iteration-->
            <Px1DilatAlti>  2    </Px1DilatAlti>
            <Px1DilatPlani> 2    </Px1DilatPlani>
            <Px2DilatAlti>  2    </Px2DilatAlti>
            <Px2DilatPlani> 2    </Px2DilatPlani>

                      <!-- porting step width -->
            <Px1Pas>        ${Pas}  </Px1Pas>
            <Px2Pas>        ${Pas}  </Px2Pas>
                      <!-- default resolution for the resolution of the
                      grid used in the spatial regularization -->
```

```
            <SsResolOptim> 4 </SsResolOptim>
         </EtapeMEC>

         <EtapeMEC> <!-- first iteration at Zoom2 -->
            <DeZoom > 2 </DeZoom>
            <Px1Pas>   0.8  </Px1Pas>               <!-- overwrite defaults -->
            <Px2Pas>   0.8  </Px2Pas>               <!-- overwrite defaults -->
            <Px1Regul> 0.5    </Px1Regul>           <!-- overwrite defaults -->
            <Px2Regul> 0.5   </Px2Regul>            <!-- overwrite defaults -->
            <SsResolOptim> 16 </SsResolOptim><!-- overwrite defaults -->
         </EtapeMEC>

         <EtapeMEC> <!-- 2nd iteration at full resolution -->
            <DeZoom > 1 </DeZoom>
            <Px1Pas>   0.4  </Px1Pas>
            <Px2Pas>   0.4  </Px2Pas>
            <Px1Regul> 0.3    </Px1Regul>
            <Px2Regul> 0.3   </Px2Regul>
            <SsResolOptim> 8 </SsResolOptim>
         </EtapeMEC>
         <EtapeMEC>
            <DeZoom > 1 </DeZoom> <!-- 3rd iteration at full resolution -->
            <Px1Pas>   0.2  </Px1Pas>
            <Px2Pas>   0.2  </Px2Pas>
            <Px1Regul> 0.3    </Px1Regul>
            <Px2Regul> 0.3   </Px2Regul>
            <SsResolOptim> 8 </SsResolOptim>
         </EtapeMEC>
        <EtapeMEC>
            <DeZoom > 1 </DeZoom> <!-- 4th iteration at full resolution -->
            <Px1Pas>   0.1  </Px1Pas>
            <Px2Pas>   0.1  </Px2Pas>
            <Px1Regul> 0.3    </Px1Regul>
            <Px2Regul> 0.3   </Px2Regul>
            <SsResolOptim> 8 </SsResolOptim>
         </EtapeMEC>

                  <EtapeMEC>
            <DeZoom > 1 </DeZoom> <!-- 5th iteration at full resolution -->
            <Px1Pas>   0.05  </Px1Pas> <!-- 1/20th pixel precision -->
            <Px2Pas>   0.05  </Px2Pas> <!-- 1/20th pixel precision -->
         </EtapeMEC>

    </Section_MEC>

    <Section_Results >
        <GeomMNT> eGeomPxBiDim </GeomMNT>
    </Section_Results>

   <Section_WorkSpace >
      <WorkDir >  ThisDir </WorkDir>
      <TmpMEC>    ${Dir} </TmpMEC>
      <TmpResult> ${Dir} </TmpResult>
      <TmpPyr>  ${Pyr}  </TmpPyr>
      <ByProcess>  ${MMNbProc} </ByProcess>

      <NbCelluleMax> 8e7 </NbCelluleMax> <!-- max. number of pixel used in the regularization
-->

      <SzRecouvrtDalles> 50 </SzRecouvrtDalles> <!-- tile overlap -->
      <SzDalleMin> 500 </SzDalleMin>               <!-- min. tile size -->

      <DefTileFile>100000</DefTileFile>

     </Section_WorkSpace>

    <Section_Vrac> </Section_Vrac>
</ParamMICMAC>
```

5 OUTLOOK/EVOLUTION OF THE TOOLKIT

5.1 STOCHASTIC CHANGE DETECTION

The current version of the service does not scale for large data sets and regions of interests have to be selected by the user. On large input data sets the service may exceed the available memory and crash. This issue will be resolved in a future release of the algorithm in order to deal with large size inputs. To do so, we plan to use the MapReduce framework.

In addition we will investigate a locally adaptive version of the change detection by integration of Kriging interpolation for a local computation of Q_{yy} and the variances.

5.2 TOPOLOGICAL CHANGE DETECTION

Future releases for this service will include:

- **V1.2**: Porting on Linux;
- **V2:** Dealing with triangulations (.ply);
- **V3:** Parallelization of the algorithms.

5.3 DISPLACEMENT MEASUREMENT USING DSM/DTM/DEM AND OPTICAL IMAGES

The following further developments are targeted to extend the functionalities currently provided by service 60 within the change detection toolkit.

- **V2**
  - Parallelization of the algorithms to comply with the IQmulus Cloud architecture;
  - Enhance robustness of the algorithms through consistency checks among time-series analysis
  - Inversion of 3D displacement from multiple views (e.g., video cameras, satellite stereo pairs, etc.)
- **V3**
  - Derivation of physical parameters from 3D displacement fields.

5.4 LINKS WITH OTHER SERVICES AND WORK PACKAGES

This section briefly provides a perspective on possible links with other services and the development carried out in other IQmulus work packages.

5.4.1 Stochastic Change Detection

In order to obtain intersected, co-registered and interpolated input images links with the following previously developed services should be envisaged:

1) Coarse registration (service #14)
2) Resampling (service #35)
3) Data intersection (service #12)

For displaying 3D input data, we can benefit from the quick visualization service (service # 16).

5.4.2 Topological Change Detection

Regarding the land showcase 1.2.2_SC2_1, a combination of the services 44, 45 and 64 could be used for studying the temporal evolution of maxima of a rainfall field. Roughly, for a distance map the idea is to select maximum points associated with high persistence, and then to track their movements within a sequence of distance maps obtained from a collection of consecutive rainfall maps.

5.4.3 Displacement Measurements using DSM/DTM/DEM and Optical Images

Regarding the infrastructure the most straightforward way to exploit the IQmulus Cloud with service 60 would be to allow for makefile parallelization on the Cloud or ghosting of a single machine. If this is not feasible the code will require major revisions to port the current implementation into the MapReduce framework.

The visualization and post-processing of the derived displacement fields currently make use of code developed with the R graphics engine. Though the implemented functions provide accurate and visually appealing results and require only minimal user interaction (Figure 12, Figure 14, Figure 15), they are not optimized in terms of speed, and especially memory consumption remains a major issue. Furthermore, basic features such as interactive changes of the color scales and zoom functions are currently missing. The provided functions could therefore serve as a base for further developments for the partners working on visualization in WP5. Of particular interest might be a dynamic visualization of the obtained vector fields and an exploitation of the multi-resolution outputs of the algorithms to optimize the computational load.

Service 53 could provide additional constraints on the vertical components of the deformation and could be combined with service 60 to derive full 3D displacement fields.

6 CONCLUSIONS

The first 18 months of Task 4.5 were dedicated to the development of three services addressing the detection of horizontal, vertical and topological changes among bi-temporal 2.5D gridded data sets. They partially comprise capabilities to handle large datasets through internal tiling and multi-core processing but further work is required to guarantee that all services scale to raster data sets that amount typically to several Gigabytes. The following computational bottlenecks have been identified regarding the existing services and will be addressed by further developments during the 12 project months to come:

- Enhance scalability of service 45 & 53 for parallel processing of large raster data sets and porting to Linux 64 bit;
- Implementation and testing of Service 60 in the IQmulus Cloud environment;
- Adaptation of service 45 to work on triangulated point clouds.

Regarding analytical functionalities it is foreseen to extend Service 60 in order to extract 3D displacement vectors from stereo or multi-view data sets and enable combinations with pointwise ground measurements to extrapolate physical parameters.

While the toolbox comprises useful techniques for the analysis of bi-temporal datasets, the analysis of time series (in particular satellite images) has not been addressed yet and should be tackled during the next year of the project.

7 REFERENCES

Barisin, I., Leprince, S., Parsons, B., & Wright, T. (2009). Surface displacements in the September 2005 Afar rifting event from satellite image matching: Asymmetric uplift and faulting. *Geophysical Research Letters, L07301*, 6

Bauer, U., Kerber, M., & Reininghaus, J. (2013). Distributed computation of persistent homology. *ArXiv pre-prints*

Bauer, U., Kerber, M., & Reininghaus, J. (To appear). Clear and compress - Computing persistent. In, *TopoInVis 2013*

Bauer, U., Lange, C., & Wardetzky, M. (2012). Optimal Topological Simplification of Discrete Functions on Surfaces. *Discrete & Computational Geometry, 47*, 347-377

Berthier, E., Vadon, H., Baratoux, D., Arnaud, Y., Vincent, C., Feigl, K.L., Rémy, F., & Legrésy, B. (2005). Surface motion of mountain glaciers derived from satellite optical imagery. *Remote Sensing of Environment, 95*, 14-28

Carlsson, G., Zomorodian, A., Collins, A.D., & Guibas, L.J. (2005). Persistence Barcodes for Shapes. *International Journal of Shape Modeling, 11*, 149-188

Chazal, F., Cohen‐Steiner, D., Guibas, L.J., Mémoli, F., & Oudot, S.Y. (2009). Gromov‐Hausdorff Stable Signatures for Shapes using Persistence. In, *Computer Graphics Forum* (pp. 1393-1403): Wiley Online Library

Delacourt, C., Allemand, P., Casson, B., & Vadon, H. (2004). Velocity field of the "La Clapière" landslide measured by the correlation of aerial and QuickBird satellite images. *Geophysical Research Letters, 31*, L15619

Deseilligny, M.-P., Belveaux, J., Choqueux, G., Deveau, M., & Girod, L. (2013). MicMac, Apero and Other Beverages in a Nutshell. In (p. 275). ENSG - Marne-la-Vallée

Edelsbrunner, H., & Harer, J. (2010). *Computational topology: An introduction*. Providence, RI: American Mathematical Society

Feigl, K.L., Sarti, F., Vadon, H., McClusky, S., Ergintav, S., Durand, P., Bürgmann, R., Rigo, A., Massonnet, D., & Reilinger, R. (2002). Estimating slip distribution for the Izmit mainshock from coseismic GPS, ERS-1, RADARSAT, and SPOT measurements. *BULLETIN OF THE SEISMOLOGICAL SOCIETY OF AMERICA, 92*, 138-160

Fitch, A.J., Kadyrov, A., Christmas, W.J., & Kittler, J. (2002). Orientation Correlation. In, *British Machine Vision Conference* (pp. 133–142)

Franzetti, M., Le Roy, P., Delacourt, C., Garlan, T., Cancouët, R., Sukhovich, A., & Deschamps, A. (2013). Giant dune morphologies and dynamics in a deep continental shelf environment: example of the banc du four (Western Brittany, France). *Marine Geology, 346*, 17-30

Heid, T., & Kääb, A. (2012). Evaluation of existing image matching methods for deriving glacier surface displacements globally from optical satellite imagery. *Remote Sensing of Environment, 118*, 339-355

Kääb, A. (2004). Mountain glaciers and permafrost creep. Methodical research perspectives from earth observation and geoinformatics technologies. Habilitation thesis, . In, *Department of Geography* (p. 205): University of Zurich

Kääb, A., & Vollmer, M. (2000). Surface Geometry, Thickness Changes and Flow Fields on Creeping Mountain Permafrost: Automatic Extraction by Digital Image Analysis. *Permafrost and Peroglacial Processes, 11*, 315–326

Leprince, S., Barbot, S., Ayoub, F., & Avouac, J.P. (2007). Automatic and Precise Orthorectification, Coregistration, and Subpixel Correlation of Satellite Images, Application to Ground Deformation Measurements. *Geoscience and Remote Sensing, IEEE Transactions on, 45*, 1529-1558

Lewis, R.H., & Zomorodian, A. (2012). Multicore homology.

Lipsky, D., Skraba, P., & Vejdemo-Johansson, M. (2011). spectral sequence for parallelized persistence. *ArXiv pre-prints*

Necsoiu, M., Leprince, S., Hooper, D.M., Dinwiddie, C.L., McGinnis, R.N., & Walter, G.R. (2009). Monitoring migration rates of an active subarctic dune field using optical imagery. *Remote Sensing of Environment, 113*, 2441-2447

Pierrot-Deseilligny, M., & Paparoditis, N. (2006). A Multiresolution and Optimization-Based Image Matching Approach : An Application to Surface Reconstruction from Spot 5- HRS Stereo Imagery. In, *WG I/5 & I/6 Workshop on Topographic Mapping from Space (with Special Emphasis on Small Satellites)*. Ankara, Turkey

Rosu, A.-M., Pierrot-Deseilligny, M., Delorme, A., Binet, R., & Klinger, Y. (2014) Measurement of ground displacement from optical satellite image correlation using the free open-source software MicMac. *ISPRS Journal of Photogrammetry and Remote Sensing*, in press

Scherler, D., Leprince, S., & Strecker, M.R. (2008). Glacier-surface velocities in alpine terrain from optical satellite imagery - Accuracy improvement and quality assessment. *Remote Sensing of Environment, 112*, 3806-3819

Vadon, H., & Massonnet, D. (2000). Earthquake displacement fields mapped by very precise correlation. Complementarity with radar interferometry. In, *Geoscience and Remote Sensing Symposium, 2000. Proceedings. IGARSS 2000. IEEE 2000 International* (pp. 2700-2702 vol.2706)

Zheng, Y., Gu, S., Edelsbrunner, H., Benfey, C.T., & Philip (2011). Detailed Reconstruction of 3D Plant Root Shape. In, *IEEE International Conference on Computer Vision (ICCV)* (pp. 2026 - 2033)

8 APPENDIX – SERVICE INFORMATION TABLES

<table>
<tr><th colspan="5">IQmulus Service information</th></tr>
<tr><th>Name of the metadata</th><th colspan="2">Content expected</th><th>Motivation/comments</th><th>INSPIRE</th></tr>
<tr><td>Service Acronym</td><td colspan="2">Service 45 Topological Change Detection</td><td>Unique identifier of the service; necessary to call it within user-defined workflows</td><td>2.2.1.1 Resource Title (mandatory)</td></tr>
<tr><td>Description</td><td colspan="2">The algorithm performs a topological analysis (0th persistence) of a distance map obtained from two co-registered gridded point clouds (GeoTIFF). Maxima, minima and saddles of such map are used to detect its topological changes, and rank them by importance. Also, points at which topological changes occur are detected. Possible adaptation to triangulations (ply) will be considered.</td><td>Brief textual description of the service: what it provides, what it can be used for. This text could be used as a short “help text” in the User Interfaces of IQmulus</td><td>2.2.1.2 Abstract (mandatory)</td></tr>
<tr><td rowspan="3">Service functionality</td><td>Input: <data representation and format></td><td>•Gridded point clouds (GeoTIFF);
•Triangulations (.ply, planned for release v2)</td><td rowspan="3">Include here the input/output of the service, the name of the functionality (e.g., registration, fusion), and input parameters (if any). In the future, we may consider defining a taxonomy of the functionalities to harmonize the terminology used to fill this field.</td><td>-</td></tr>
<tr><td>Input parameters: [optional]</td><td>• Persistence threshold to filter out irrelevant topological changes;
• [optional] NoDataValue, in case part of the input does not have to be considered.</td><td>-</td></tr>
<tr><td>Output: <data representation and format></td><td>• List of topological changes (persistence diagram, .mat 2D array);
• Total persistence (a measure of the “amount” of topological changes, real value);
• List of 2D points at which topological changes occur (shape file).
• Possibly,</td><td>-</td></tr>
</table>

	Functionality of the service: <text>	Data change detection		*2.2.2.2 Classification of spatial data services (mandatory)*
Algorithm	Union-find data structure for: • Topological features extraction (0th persistence); • detection of 2D points characterizing topological changes.		*Explanation of the algorithm used to provide the expected functionality; alternative algorithms may be considered for the same functionality to provide adaptivity to the context in which the services in run (eg, dataset, size of the geographical area)*	-
Implementation details	**Implementation language**	C++	*Include information related to the implementation of the service, such as language (e.g., C, C++, etc); dependencies with other libraries (e.g., ANN library); constraints on the operating systems, and visualization modalities of the output.*	-
	Dependencies with other libraries (when relevant, indicate required version**)**	• Shapefile C/C++ Library; • LibTIFF C/C++ Library; • GeoTIFF C/C++ Library;		-
	Operating system	Windows, Linux		-
	Source code availability [yes | no]	Will be available		
Tool chain	**Operating System [Windows | GNU/Linux | Mac OS]**	Windows (Linux version planned for release V1.2)		
	Operating System Version	WINDOWS 7 ENTERPRISE N 64bit (SP1)		
	Operating System Architecture [32 bit | 64 bit]	64 bit		
IQmulus Data	**Available IQmulus input data**: 27 (Regione Liguria); 36, 37, 42 (CNR -IMATI).		*If there are examples of data that could serve as an example, then include here their identifiers as in the data table in eRoom (useful to test the service)*	-

	Max data set/tile size that can be handled by the service	(6071 x 5416) GeoTIFF on intel Core i7-3770 CPU @ 3.40 GHz, RAM 8.00 GB, 64bit	
Service characteristics	**Accuracy:** machine precision for the distance map (it depends on the height function).	*These fields are necessary to document all the characteristics of the services that are important to assess the quality of the results. Also, these fields could be used to select a specific service among more services that implement the same functionality but with different characteristics. See the following box.*	-
	Robustness: the approach is robust to perturbation of the distance map; the chosen connectivity directly acts on the considered topology, hence this may affect final results.		-
	Computational time in relation to data size: The computational cost of the service for the detection of the topological changes is $O(n \cdot \alpha(n))$, where n is the number of points in the input gridded point cloud, and α is the inverse of the Ackermann function.		-
	Locality/globality of the algorithm: • The service computational cost should allow for the processing of large data sets; • Recent works show the possibility of introducing a distributed computation of persistence.		-
Alternatives	Service #25: *Change detection using point clouds;* Service #53: *Stochastic change detection.*	*List other services (if any) that have the same functionality, have the same input/output but use a different algorithm or have different features*	-
Related use cases and scenario (Land, Marine, Urban)	The Land Showcase - User Story 1.2.2_SC2_1;	*Mention the user stories related to the usage of the service (see D4.1.1) and related use cases uploaded on Red Mine*	*-mandatory*
Responsible Partner	Andrea Cerri, andrea.cerri@ge.imati.cnr.it (CNR-IMATI)	*Partner ID and responsible person (include email)*	*2.2.10 Responsible organisation (mandatory)*
Involved Partners	Silvia Biasotti (CNR-IMATI), Michela Spagnuolo (CNR-IMATI)		-

IQmulus Service information				
Name of the metadata	**Content expected**		**Motivation/comments**	**INSPIRE**
Service Acronym	Service 53 Stochastic Change Detection		*Detecting changes that are significant given the quality of the observations in both epochs.*	**INSPIRE**
Description	This service evaluates if grid point wise differences are so large that a change is likely, given the variance of the input data.			*2.2.1.1 Resource Title (mandatory)*
Service functionality	**Input: <data representation and format>**	Two GeoTIFF format digital surface models with the same support. This means that both input files consist of the same grid points possibly including some NaN values.	*2.2.1.2 Abstract (mandatory)* - - -	
	Input parameters: *[optional]*	**α** level of significance **σ_{h1}** and **σ_{h2}** of the input data		
	Output: <data representation and format>	Geotiff file, for each grid point two attributes are determined, a 0/1 binary value indicating stability vs. change and a test statistic **T_q**. which is the distance to model expressing stability in the VC-metric		
	Functionality of the service: <text>	See description.		
Algorithm	Input: For each grid-point two, say, height values and their variances are given (**h_1, σ_{h1}^2**) and (**h_2, σ_{h2}^2**); 1) Calculate variance-covariance matrix of the observations **$Q_{yy} = [\sigma_{h1}^2, 0$** **$0, \sigma_{h2}^2]$** 2) Design matrix **$A = [1,1]^T$** 3) Calculate the common height **$y = (A^T * Q_{yy}^{-1} * A)^{-1} * A^T * Q_{yy}^{-1} * [h_1, h_2]^T$** 5) Vector of residuals **$e = [h_1, h_2]^T - [y, y]^T$**			*2.2.2.2 Classification of spatial data services (mandatory)*

	6) Calculate test statistic $\mathbf{T_q = e^T * Q_{yy}^{-1} * e}$ 7) Evaluate $\mathbf{T_q}$ against critical value $\boldsymbol{\kappa_\alpha}$ Here the critical value κ_α is defined as the solution of the equation **$1 - cdf(\chi^2(q,0), x) = \alpha$**, with **$q=1$** **$\chi^2(q,0)$** denotes the central Chi squared distribution with **q** degrees of freedom			
Implementation details	**Implementation language**	C/C++	-	-
	Dependencies with other libraries (when relevant, indicate required version**)**	PCL, Boost, Eigen, OpenGL, VTK, LibTIFF, LibgeoTIFF libraries will be needed.	-	-
	Operating system	The algorithm will be developed for these operating systems; Windows 7, 64 bits and Linux	-	-
	Source code availability [yes | no]	yes	-	
Tool chain	**Operating System [Windows | GNU/Linux | Mac OS]**	Windows		
	Operating System Version	7 or 8		
	Operating System Architecture [32 bit | 64 bit]	64 bit		
IQmulus Data	**Available IQmulus input data**: <ID of the dataset as in the eRoom tables>		(1) UBO – Bathymetry in Brittany (ID-12-13) (2) AHN-2 (internal data set) (3) Dutch coastal zone stones (internal data set) *(4)* Laser scan of a desk (internal data set) *(5)* IMATI – Italy, Liguria	
	Max data set/tile size that can be handled by the service		*1000x1000 pixel region is recommended for now.*	-
Service characteristics	**Accuracy:** The significance of the change is indicated by the test statistic $\mathbf{T_q}$.			

	Robustness: Reliability is verified by testing several other point cloud data sets.		-
	Computational time in relation to data size: Complexity is linear, O(n). Couple of minutes computational time is expected for approximately 1 million grid points		-
	Locality/globality of the algorithm: It is a local algorithm, just working on individual grid points.		-
Dependencies	The service may require the support of two other services to obtain the required input; 1) Coarse registration (service #14) 2) Resampling (service #35) 3) Data intersection (service #12)		-
Alternatives	There is no commercial/non-commercial solution available for this service.		-
Related use cases and scenario (Land, Marine, Urban)	Relevant for Marine, Land and Urban show cases.		*-mandatory*
Responsible Partner	TUDelft, Beril Sirmacek, b.sirmacek@tudelft.nl	*Partner ID and responsible person (include email)*	*2.2.10 Responsible organisation (mandatory)*
Involved Partners	• TUDelft, Roderik Lindenbergh, R.c.Lindenbergh@tudelft.nl (algorithm development support) • TUDelft, Jinhu Wang, Jinhu.wang@tudelft.nl (testing)		-

IQmulus Service information				
Name of the metadata	**Content expected**		**Motivation/comments**	**INSPIRE**
Service Acronym	Service 60 – 2D Displacement measurement using DSM/DTM/DEM and optical images		*Unique identifier of the service; necessary to call it within user-defined workflows*	*2.2.1.1 Resource Title (mandatory)*
Description	2D Displacement measurement using DSM/DTM/DEM and optical images using sub-pixel image cross-correlation with spatial regularization.		*Brief textual description of the service: what it provides, what it can be used for. This text could be used as a short "help text" in the User Interfaces of IQmulus*	*2.2.1.2 Abstract (mandatory)*
Service functionality	**Input: <data representation and format>**	• 2 gridded point clouds GeoTIFF) or 2D images (GeoTIFF) with the same pixel size	*Include here the input/output of the service, the name of the functionality (e.g., registration, fusion), and input parameters (if any). In the future, we may consider defining a taxonomy of the functionalities to harmonize the terminology used to fill this field.*	-
	Input parameters: *[optional]*	• *window Size*; • *search radius;* • *resolution* • *correlation threshold* • *regularization factor*		-
	Output: <data representation and format>	3 raster per resolution level (GeoTIFF): • X displacement • Y displacement, • Correlation coefficient		-
	Functionality of the service: <text>	Quantification of displacement between diachronic datasets		*2.2.2.2 Classification of spatial data services*

				(mandatory)
Algorithm	• Window based image-cross-correlation using normalized cross-correlation and a term for the smoothness of the displacement field as an objective function.		*Explanation of the algorithm used to provide the expected functionality; alternative algorithms may be considered for the same functionality to provide adaptivity to the context in which the services in run (eg, dataset, size of the geographical area)*	-
Implementation details	**Implementation language**	C++, R	*Include information related to the implementation of the service, such as language (e.g., C, C++, etc); dependencies with other libraries (e.g., ANN library); constraints on the operating systems, and visualization modalities of the output.*	-
	Dependencies with other libraries (when relevant, indicate required version**)**	• GDAL (1.10.0-1) • Tcl-tk/ tk-dev (8.5) • GNU make (3.81.-8.10) • GCC (4.6,3-1) • Imagemagick (6.6.9.7) • libimage-exiftool-perl • exiv2 (0.22-2) • libgeo-proj4-perl R (=>3.0) • R packages (raster, rasterVis, rgdal, XML, TIFF, etc.)		-
	Operating system	Linux		-
	Source code availability [yes | no]	yes		
Tool chain	**Operating System [Windows | GNU/Linux | Mac OS]**	GNU Linux		
	Operating System Version	Ubuntu 12.04 LTS		
	Operating System Architecture [32 bit | 64 bit]	64 bit		

IQmulus Data	**Available IQmulus input data**: • 8, 9, 12, 13 (UBO) • 39 (UBO)	*If there are examples of data that could serve as an example, then include here their identifiers as in the data table in eRoom (useful to test the service]*	-
	Internal tiling, no known constrains regarding the size of the input dataset		
Service characteristics	**Accuracy:** Sub-pixel precision to approximately $1/10^{th}$ of pixel on noise free data	*These fields are necessary to document all the characteristics of the services that are important to assess the quality of the results. Also, these fields could be used to select a specific service among more services that implement the same functionality but with different characteristics. See the following box.*	-
	Robustness: High robustness compared to stat-of-the-art correlation in the frequency domain. Higher regularization can be enforced to compensate noise. Fails in areas with no texture (e.g. snow fields, shadows) and when no homologous surface features are preserved between the two time steps.		-
	Computational time in relation to data size: By default in the order of $O(n)$, but it can be significantly reduced by using and implemented hierarchical scheme, using smaller search window size and search radius, and constraining the precision to ¼ pixel.		-
	Locality/globality of the algorithm: • Uses makefile parallelisation adapted for parallel processing on a single machine • Makefile parallelization on the cloud still needs to be tested		-
Alternatives	none	*List other services (if any) that have the same functionality, have the same input/output but use a different algorithm or have different features*	-
Related use cases and scenario (Land, Marine, Urban)	• Land Showcase - User Story 1.2.2_SC2_1; • Marine Showcase • Use cases ID as in RedMine: 1095,1040,1043	*Mention the user stories related to the usage of the service (see D4.1.1) and related use cases uploaded on Red Mine*	*-mandatory*
Responsible Partner	UBO, André Stumpf, andre.stumpf@univ-brest.fr	*Partner ID and responsible person (include email)*	*2.2.10 Responsible organisation (mandatory)*
Involved Partners	Christophe Delacourt (UBO), Helen Piete (UBO), Romain Cancouet (UBO)		-